photo-beam sensors (25-mm intervals for the horizontal axis and 150 mm for the vertical axis) for 60 min.

Context fear learning and latent inhibition

The test paradigm of contextual conditioning was based on the work by Zhang et al. (39). The rats receiving ZD1839 or vehicle were transported to the laboratory at least 30 min prior to the fear-conditioning procedure. Rats were placed in a shock chamber with a stainless steel grid floor (21.5 cm W × 20.5 cm D × 30 cm H; Ohara Medical Industry, Inc., Tokyo) for 2 min to monitor baseline movement and freezing behavior. The rats were then exposed to a tone cue for 30 s (conditioned stimulus, CS: 60 dB, 10 Hz) together with 2-s 0.8-mA electric shocks (un-conditioned stimulus, US; given twice with a 1-min interval). One day after conditioning, the rats were returned to the same chamber and exposed to the same CS. The time spent freezing after the start of the CS was recorded by a video camera and averaged every 30 s with the aid of imaging software (Ohara Medical Industry, Inc.). The rats were divided into two groups; a preexposure group and a non-preexposure group. Animals in the non-preexposure group received the conditioning alone as detailed above. The rats in the preexposure group, on the other hand, were placed in the shock chamber for 20 min and preexposed to the same contextual cue (CS) but did not receive the electric stimuli (US). This was performed one day prior to the conditioning. Latent inhibition score was calculated as follows:

Latent inhibition score (%) = [(mean performance of NPE group − performance of each PE rat) / (mean performance of NPE group)] × 100

Statistical analyses

The results are expressed as means ± S.E.M. Statistical differences of behavioral data were determined by analysis of variance (ANOVA). When univariate data were obtained from two groups, a two-tailed *t*-test was used for comparison. Behavioral scores were initially subjected to a multiple ANOVA using lesion (two levels), drug treatment (two or three levels), and/or preexposure to CS (two levels) as between-subjects factors and prepulse magnitude (three levels) as a within-subjects factor. We estimated the interaction of a within-subjects factor with a between-subjects factor by multivariate analysis of variance with Pilli compensation. As the initial analyses yielded a significant factorial interaction, the data were separated for the final analyses. We used Fisher's LSD test for post hoc testing with multiple comparisons. Correlations between pulse-alone startle and PPI were examined by Pearson correlation analysis. A P value less than 0.05 was regarded as statistically significant. Statistical analyses were performed using Stat view software (SAS Institute, Inc., Cary, NC, USA) and SPSS 11.0 for Windows (SPSS, Inc., Tokyo). N values in parentheses represent the number of animals used in each study.

Results

Pharmacological influences of ZD1839 on sensorimotor gating in the VHL model

Lesioning the ventral hippocampus of neonate rats produces abnormal behavioral traits that are implicated in schizophrenia and its related psychiatric diseases, for example, PPI and latent inhibition of learning (21, 22, 24). We performed neonatal hippocampal lesioning or sham operations in neonatal rats (18) and allowed the rats to reach the young adult stage (postnatal day 54 – 60). Using this animal model for schizophrenia, we examined three quinazoline derivatives, ZD1839, OSI-774, and PD153035, which contain the core structure of 4-amino-6,7-dimethoxy-quinazoline and inhibit the tyrosine kinase activity of the ErbB1 receptor (Fig. 1). Almost all the rats receiving VHL as neonates exhibit bilateral or unilateral

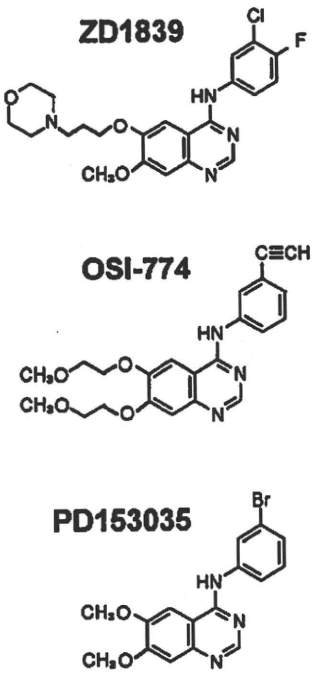

Fig. 1. Chemical structures of three tyrosine kinase inhibitors for ErbB1. Three quinazoline derivatives that inhibit tyrosine kinase activity of the EGF receptor (ErbB1) and contain the common core structure of 4-amino-6,7-dimethoxy-quinazoline: ZD1839 [gefitinib, 4-(3-chloro-4-fluorophenylamine)-7-methoxy-6(3-(4-morpholinyl)-quinazoline], OSI-774 [tarceva, 4-(3-ethynylphenylamine)-6,7-bis(2-methoxyethoxy)-quinazoline], and PD153035 [4-(3-bromophenylamine)-6,7-dimethoxy-quinazoline].

cell loss in the ventral hippocampus (Fig. 2A).

First, we subchronically administered ZD1839 (1 mg/mL; 0.5 μg/h) or vehicle (10% DMSO) to the lateral cerebroventricle of adult rats receiving VHL or sham operations as the permeability of the blood-brain barrier to these quinazoline derivatives is limited (40). We chose the dose of 0.5 μg ZD1839/h since our preliminary study indicated that this dose shows the maximum efficacy in another animal model for schizophrenia (M. Mizuno, unpublished data). At 5 – 7 days after drug administration, we measured the startle responses to a 120-dB tone and PPI levels in these rats (Fig. 2B). The pulse-alone startle responses (120 dB) were significantly altered by VHL [$F(1,52) = 11.1$, $P = 0.016$, ANOVA] but not by drug administration [$F(1,52) = 3.77$, $P = 0.058$]. There was also a significant interaction between VHL and drug [$F(1,52) = 7.87$, $P = 0.007$]. Post-hoc analysis indicated that ZD1839 administration significantly increased pulse-alone startle amplitudes in sham-operated controls but not in VHL rats.

We measured PPI levels and found that subchronic infusion of ZD1839 ameliorated PPI deficits of VHL rats (Fig. 2C). A three-way ANOVA was conducted with between-subjects factors of treatment (VHL and sham-operate) and drug (ZD1839 and vehicle) and a within-subjects factor of prepulse intensities (75, 80, and 85 dB). This analysis revealed significant main effects of VHL [$F(1,52) = 63.1$, $P < 0.001$] and drug [$F(1,51) = 16.6$, $P < 0.001$] and a significant interaction between VHL and drug [$F(2,104) = 7.13$, $P = 0.010$]. We interpret from these data that ZD1839 had a differential effect on VHL and sham-operated animals. Post-hoc analysis revealed that ZD1839 administration significantly increased PPI levels of VHL rats for all prepulse intensities.

As the amplitude of pulse-alone startle is the denominator of the %PPI formula, the increase of VHL rats in pulse-alone startle might be responsible for the observed decrease in %PPI (36, 37). To test this possibility, we additionally prepared eight ZD1839-treated VHL rats and eight vehicle-treated VHL rats to enhance the statistical power. Individual PPI and startle values for VHL rats and control animals were re-analyzed by the linear regression method (Fig. 3A). When PPI levels for 80-dB prepulse were plotted *versus* the magnitude of the pulse-alone startle, there were significant and insignificant positive correlations between pulse-alone startle and PPI

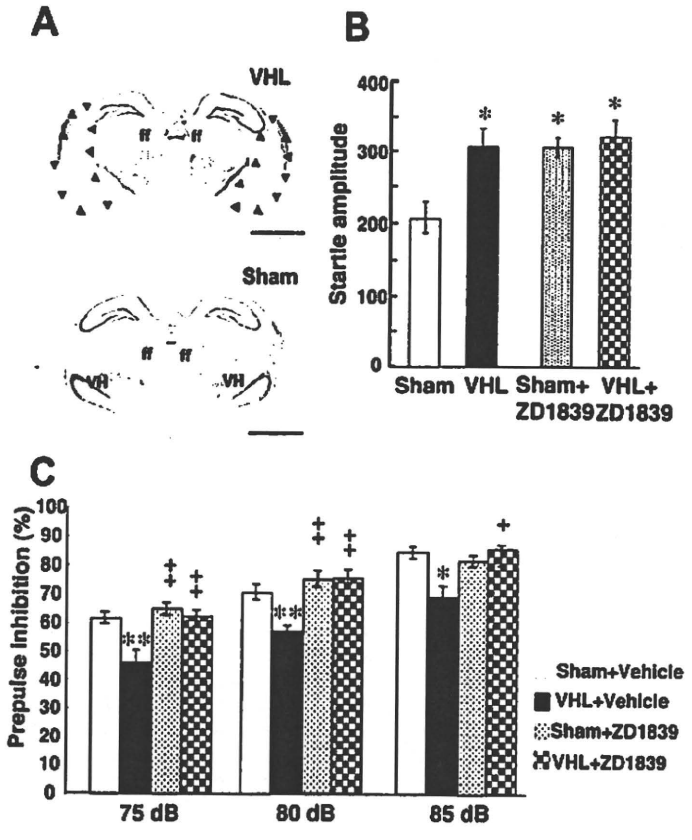

Fig. 2. Brain histology and prepulse inhibition of rats receiving ventral hippocampal lesioning as neonates. A) Coronal brain sections were prepared from adult rats receiving VHL as neonates and stained with cresyl violet. Arrowheads point to the ventral hippocampal (VH) regions containing hippocampal loss (CA3-CA4) in a typical section 4.5-mm posterior from the bregma; ff, fasciculus fissure. Histological analysis of 48 rats showed that 25 rats received bilateral damages of the hippocampus, 18 rats received unilateral damage, and 5 rats had no damage. Some rats with large hippocampal lesion(s) carried unilateral extrahippocampal damages; one lateral thalamus and three amygdala. Data from the rats not receiving hippocampal damage were excluded, whereas the rats having unilateral damage exhibited PPI deficits and were included in the data analysis. Scale bars, 3 mm. B) ZD1839 (1 mg/mL, 0.5 μg/h) or vehicle (10% DMSO) was administered to the lateral cerebroventricle for 5 – 7 days. Pulse-alone startle of rats with sham-operations plus vehicle (open bar) or sham-operations plus ZD1839 (dotted bar) and rats with VHL plus vehicle (closed bar) or VHL plus ZD1839 (checked bar) was measured with a 120-dB tone as adults. C) Prepulse inhibition (PPI) of the above rats was determined in the presence of 75-, 80-, and 85-dB prepulse stimuli. Bars indicate means ± S.E.M. ($n = 10$, each). $^{*}P < 0.05$, $^{**}P < 0.01$: compared to the sham-operation plus vehicle group and $^{+}P < 0.05$, $^{++}P < 0.01$: compared to the VHL plus vehicle group (both by Fisher LSD).

in these experimental groups (Fig. 3A). We did not obtain any sign of negative correlation between these indices. Even when we matched the amplitude of pulse-alone startle among groups, choosing VHL rats (n = 10) having the lower pulse-alone startle responses (Fig. 3B), we still observed the same effects of VHL and ZD1839 on PPI (Fig. 3C). Thus, we conclude that ZD1839 ameliorates the PPI deficits irrespective of pulse-alone startle.

ZD1839 effects on tone-dependent learning and latent inhibition in the VHL model

We evaluated the effect of the ErbB1 inhibitor ZD1839 on fear learning and latent inhibition by subjecting lesioned and sham-operated rats to context-associated fear conditioning in the presence or absence of preexposure to the CS (39). The initial three-way ANOVA on freezing behavior during conditioning consisted of between-subjects factors of lesion (+/−), inhibitor (+/−), and preexposure to CS (+/−). This analysis did not reveal any significant main effects [$F(1,56) = 0.002 - 1.106$, $P = 0.297 - 0.966$] or interactions between the factors [$F(1,56) = 0.052 - 2.32$, $P = 0.133 - 0.821$], suggesting that neither hippocampal lesioning, drug administration, nor preexposure to CS altered shock sensitivity. In contrast, a three-way ANOVA on learning scores revealed significant interactions between lesion and preexposure [$F(1,56) = 6.482$, $P = 0.013$], between lesion and drug [$F(1,56) = 6.482$, $P = 0.0137$], and between preexposure and drug [$F(1,56) = 7.688$, $P = 0.0075$]. The interaction between lesion and preexposure corroborates a previous finding that neonatal hippocampal lesioning alters latent inhibition scores of fear learning (24).

We then separated the behavioral data by lesion status (i.e., sham-operated and lesion) and conducted indepen-

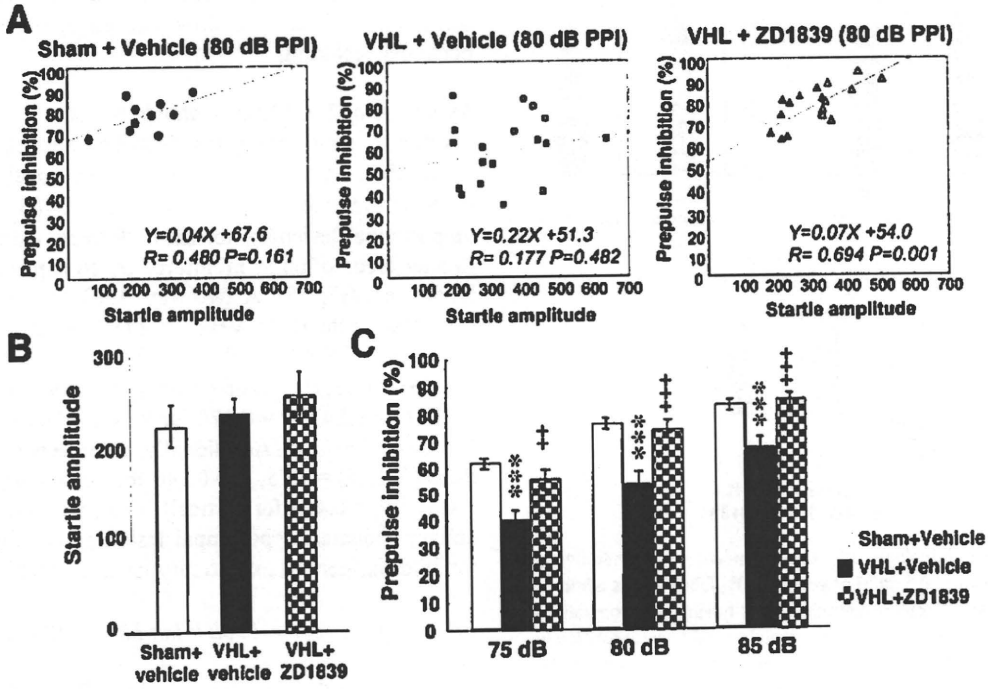

Fig. 3. Analyzing contribution of pulse-alone startle responses to prepulse inhibition in the ventral hippocampal lesion model. Sixteen VHL model rats were additionally prepared, treated with vehicle (n = 8) or ZD1839 (n = 8) at the adult stage, and subjected to the PPI test. A) We combined the data of the VHL rats with those of Fig. 2 (n = 18 total for each group). PPI levels (80-dB stimuli) of rats with sham-operation plus vehicle (closed circle), rats with VHL plus vehicle (square), and VHL plus ZD1839 (triangle) were plotted over their amplitudes of pulse-alone startle. The line of best fit was calculated by the linear regression method and presented with a broken line. Statistical correlation between pulse-alone startle and PPI was analyzed by Pearson's correlation analysis. Correlation coefficient (R) and its probability (P) are presented in each window. B) The lower pulse-alone startle scores of rats with VHL plus vehicle (closed square, n = 10) and VHL plus ZD1839 (closed triangle, n = 10) were selected to match to startle scores of rats with sham-operation plus vehicle (control, n = 10). C) PPI levels of the VHL rats, whose pulse-alone startle was matched to that of control group in panel B, was re-evaluated and plotted. Bars indicate means ± S.E.M. (n = 10 each). $^{***}P < 0.001$: compared to the sham-operation plus vehicle group and $^{**}P < 0.01$, $^{***}P < 0.001$: compared to the VHL plus vehicle group (both by Fisher LSD).

dent statistical analyses. A two way-ANOVA for the sham group revealed a significant main effect of preexposure [$F(1,28) = 32.29$, $P < 0.001$] but not drug [$F(1,28) = 3.72$, $P = 0.064$]. There was no significant interaction between preexposure and drug [$F(2,28) = 0.47$, $P = 0.829$] (Fig. 4A). Post-hoc comparisons detected significant effects of preexposure on learning of sham-operated animals irrespective of ZD1839 treatment. In contrast, the same analysis for the lesioned group revealed a significant main effect of drug [$F(1,28) = 22.38$, $P < 0.001$], no significant main effect of preexposure [$F(1,28) = 1.45$, $P = 0.239$], and a significant interaction between preexposure and drug [$F(1,28) = 11.20$, $P = 0.0023$] (Fig. 4B). Post-hoc comparisons in the drug-free VHL group revealed that there was no significant difference in learning scores between non-preexposure and preexposure, suggesting that neonatal hippocampal lesioning suppressed latent inhibition of fear learning. ZD1839 administration to VHL rats significantly revived the preexposure effect in the lesioned group and allowed the latent inhibition of learning to occur. In order to compare the magnitude of latent inhibition among four groups directly, we calculated ratios of the decrease in learning score that was caused by preexposure to tone cues (Fig. 4C). A two-way ANOVA with between-subjects factors of lesion (+/−) and drug (+/−) revealed significant interactions between lesion and drug for the latent inhibition ratio [$F(1,28) = 13.1$, $P = 0.0012$]. Post-hoc comparisons revealed that only the rats receiving VHL plus vehicle exhibited a lower latent inhibition ratio and that the ratio of the rats receiving VHL plus ZD1839 was indistinguishable from that of control animals. These findings suggest that the ErbB1 inhibitor ameliorates the disruption of latent inhibition caused by neonatal hippocampal lesioning.

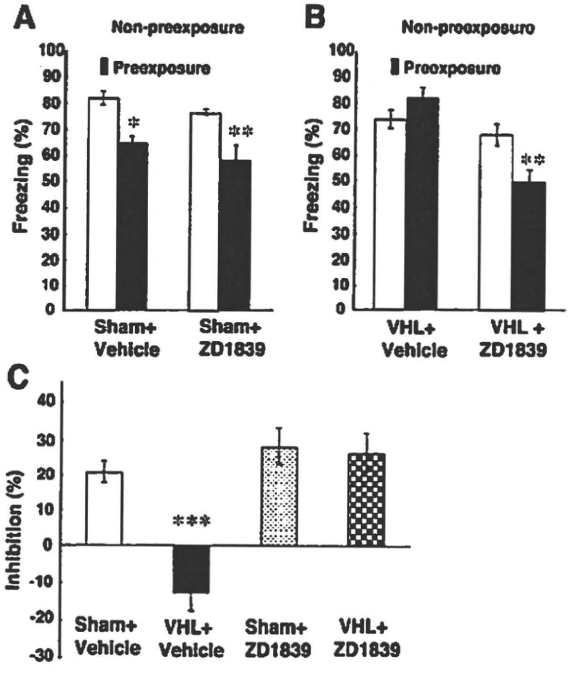

Fig. 4. Latent inhibition of tone-dependent fear-conditioning. ZD1839 (1 mg/mL, 0.5 μg/h) or vehicle (10% DMSO) was administered to the lateral cerebroventricle of rats having sham operations (Sham) or VHL for 12 days. Learning ability and latent inhibition in rats with Sham or with VHL was determined with a contextual fear conditioning procedure and compared between treatments with vehicle or ZD1839. Before the conditioning, rats in the preexposure group had repeatedly been preexposed to the same context cue without shock on day 7 (PE, n = 8, each). Rats in the non-preexposure group were directly subjected to conditioning on day 8 (NPE; n = 8, each). The data for learning performance were separated into sham-operated (A) and VHL (B) groups and analyzed separately. C) Latent inhibition of learning performance was directly compared among the four groups by calculating latent inhibition scores as follows: Latent inhibition score (%) = [(mean performance of NPE group − performance of each PE rat) / (mean performance of NPE group)] × 100. Bars indicate means ± S.E.M. (n = 7 each). $^{*}P < 0.05$, $^{**}P < 0.01$, $^{***}P < 0.001$ by Fisher LSD.

Influences of ZD1839 on motor behaviors

Prior to conditioning (as described above), the rats were subjected to a locomotor test in a novel environment to evaluate the side effects of ZD1839. Neither hippocampal lesioning nor ZD1839 treatment appeared to alter locomotion as monitored by an exploratory behavior test (Fig. 5). A two-way ANOVA revealed no significant effects of VHL or ZD1839 on horizontal movement [$F(1,16) = 0.454$, $P = 0.510$ for lesion; $F(1,16) = 1.33$, $P = 0.266$ for drug] or vertical movement [$F(1,16) = 0.842$, $P = 0.374$ for lesion; $F(1,16) = 0.517$, $P = 0.483$ for drug]. Additionally, there were no interactions [$F(1,16) = 1.45$, $P = 0.240$ for horizontal; $F(1,16) = 0.517$, $P = 0.483$ for vertical]. Thus, we conclude that neither neonatal hippocampal lesioning nor the ErbB1 inhibitor influenced exploratory locomotor activity.

Effects of the other ErbB1 inhibitors PD153035 and OSI-774

To confirm that the ameliorating effects of ZD1839 can be generalized for ErbB1 inhibitors, we tested other ErbB1 inhibitors, PD153035 and OSI-774 (33), in the PPI paradigm (Table 1). Similarly we administered these inhibitors (1 mg/mL for PD153035 and 0.1 mg/mL for OSI-774, both 0.5 μg/h) to the cerebroventricle of VHL rats using an osmotic pump and measured pulse-alone startle responses and PPI levels. A two-way ANOVA of pulse-alone startle responses with between-subjects factors of lesion (VHL and sham-operate) and drug (vehicle, PD153035, and OSI-774) revealed a main effect of lesion

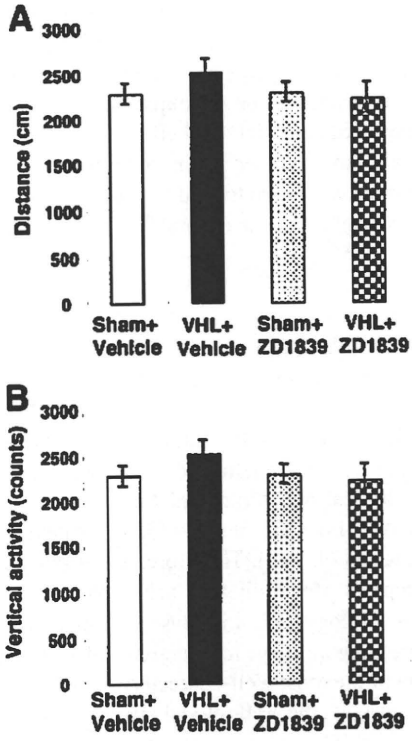

Fig. 5. Influences of ZD1839 infusion on locomotor activity. The adverse effects of VHL and ZD1839 were assessed by the locomotor activity test prior to the above fear conditioning (Fig. 4). The total number of beam crossings for horizontal movement (A) and vertical movement (rearing) (B) of the rats was monitored for 1 h in a novel environment. Bar indicates mean ± S.E.M. (n = 5 each).

on pulse-alone startle response [$F(1,54) = 10.55$, $P = 0.002$] but no significant main effect of drug [$F(2,54) = 0.482$, $P = 0.62$], which contrasts with the fact that ZD1839 increased pulse-alone startle levels of sham-operated animals (see Fig. 2B). There was no interaction between lesion and drug [$F(2,54) = 1.63$, $P = 0.205$]. We applied a three-way repeated ANOVA to PPI scores using between-subjects factors of lesion and drug and a within subject factor of prepulse intensity. This analysis revealed main effects of lesion [$F(1,54) = 14.03$, $P < 0.001$], drug [$F(2,54) = 4.48$, $P = 0.0158$], and prepulse [$F(2,108) = 176.9$, $P < 0.001$]. There was also a significant interaction between lesion and drug [$F(2,54) = 4.94$, $P = 0.0107$]. Post-hoc testing detected significant increases in PPI in the lesioned rats receiving OSI-774 and PD153035 compared to those receiving vehicle. In contrast, the drug administration did not elicit significant changes in PPI levels in control rats having sham-operations. Therefore, our results suggest that the ErbB1 inhibitors commonly ameliorate PPI deficits induced by neonatal hippocampal lesioning.

To ascertain the pharmacological action of the ErbB1 inhibitors, we determined protein levels of phospho-ErbB1 and total ErbB1 in the region surrounding the cerebroventricle, striatum, and frontal cortex (Fig. 6). A two-way ANOVA with between-subjects factors of treatment (VHL and sham-operate) and drug (vehicle, PD153035, and ZD1839) was applied to phospho-ErbB1 levels in the region surrounding the cerebroventricle. There were significant main effects of VHL [$F(1,18) = 281$, $P < 0.001$] and drug [$F(2,18) = 96.8$, $P < 0.001$] and a significant interaction between VHL and drug [$F(2,18) = 73.8$, $P < 0.001$]. The analysis for total ErbB1

Table 1. Effects of ErbB1 inhibitors on pulse-alone startle and prepulse inhibition

Treatment	Pulse alone (arbitrary units)	75-dB Prepulse (%)	80-dB Prepulse (%)	85-dB Prepulse (%)
Sham + Vehicle	227.3 ± 24.6	63.1 ± 2.2	77.0 ± 2.1	82.9 ± 1.1
Sham + OSI-774	250.1 ± 20.8	62.9 ± 2.4	75.5 ± 3.0	84.2 ± 3.0
Sham + PD153035	295.6 ± 30.9	64.9 ± 3.0	73.9 ± 2.0	83.9 ± 1.8
VHL + Vehicle	365.9 ± 38.8**	48.4 ± 2.6***	61.4 ± 4.9*	68.3 ± 3.1**
VHL + OSI-774	315.6 ± 24.1*	58.0 ± 2.7#	68.7 ± 1.6	82.0 ± 2.4##
VHL + PD153035	329.5 ± 33.6*	61.1 ± 2.8##	74.9 ± 3.4#	82.9 ± 3.2##

Vehicle (10% DMSO, 0.5 μL/h), OSI-774 (0.1 mg/mL, 0.05 μg/h), or PD153035 (1 mg/mL, 0.5 μg/h) was subchronically administered to the cerebroventricle of adult rats with sham operations (Sham) or with VHL. Pulse-alone startle response with a 120-dB tone (arbitrary units of the startle chamber) and PPI (%) with 75-, 80-, and 85-dB prepulse stimuli were measured 5 – 7 days after the start of intracerebroventricular infusion. The data represent means ± S.E.M. (n = 10). *$P < 0.05$, **$P < 0.01$, ***$P < 0.001$: compared to vehicle-receiving rats with sham operations with Fisher LSD. #$P < 0.05$, ##$P < 0.01$: compared to vehicle-receiving rats with VHL with Fisher LSD.

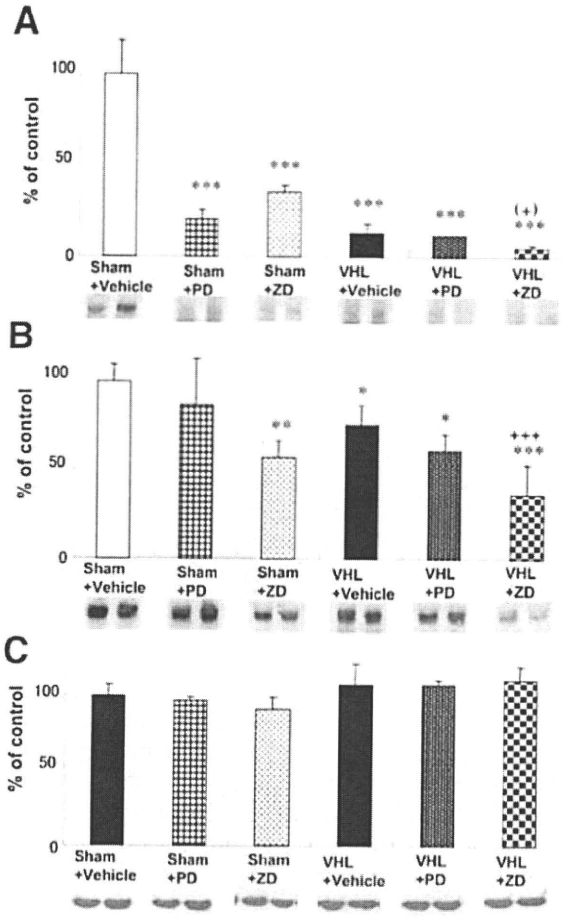

Fig. 6. Protein levels of phosphorylated ErbB1 and total ErbB1 in the region surrounding the cerebroventricle. The brain tissue homogenates were prepared from the striatum and white matter surrounding cerebroventricle of sham-operated (Sham) rats or VHL rats receiving vehicle (10% DMSO), ZD1839 (ZD; 1 mg/mL, 0.5 μg/h), or PD153035 (PD; 1 mg/mL, 0.5 μg/h) for 12 days (n = 4 rats each). Protein samples (50 μg) were separated by SDS-polyacrylamide gel electrophoresis on an 8% gel, transferred to a nylon membrane, and incubated with anti-phospho-ErbB1 and anti-ErbB1 antibodies, as well as with anti-β-actin antibodies as an internal control. Immunoblot signals for phospho-ErbB1 (A), total ErbB1 (B), and β-actin (C) were measured by densitometric analysis and are shown as means ± S.E.M. Typical blots (n = 2 lanes each) are shown in this figure. Note: β-actin levels displayed no significant differences among groups, but [$F(2,18) = 0.82$, $P = 0.457$]. *Significantly different from the sham-operated rats receiving vehicle (*$P < 0.05$, **$P < 0.01$, ***$P < 0.001$ by Fisher LSD). +Significantly or marginally different from VHL rats receiving vehicle [+++$P < 0.001$, +$P < 0.05 - 0.10$ by Fisher LSD].

also revealed significant main effects of VHL [$F(1,18) = 24.0$, $P < 0.001$] and drug [$F(2,18) = 23.8$, $P < 0.001$], but no significant interaction between VHL and drug [$F(2,18) = 0.82$, $P = 0.457$]. Post-hoc analysis revealed that ZD1839 administration significantly or marginally decreased phospho-ErbB1 and total ErbB1 levels in the region surrounding the cerebroventricle. In contrast, PD153035 only affected phospho-ErbB1 levels in the sham-operated group and total ErbB1 levels in the VHL group. Control protein, β-actin, displayed no significant differences among groups, however. Although we also explored potential basal effects of VHL on ErbB1 phosphorylation in other brain regions (striatum and frontal cortex), we failed to find any remarkable changes in ErbB1 phosphorylation or total ErbB1 levels (data not shown).

Discussion

The peptide growth factor EGF interacts with ErbB1, which forms dimeric receptor complexes with itself or ErbB2 – 4, a member of the same family of tyrosine kinase receptor (7, 9). Genetic and behavioral studies indicate pathological and biological links between schizophrenia and EGF/ErbB1 function (5, 41) or neuregulin-1/ErbB4 function (42, 43). Therefore, abnormal signals to ErbB receptors are implicated schizophrenia neuropathology or etiology (44, 45). Based on this hypothesis, we explored the antipsychotic activity of ErbB1 inhibitors in one of the most well-characterized animal models for schizophrenia, the VHL model (16, 17, 31). The brain infusion of ErbB1 inhibitors markedly decreased ErbB1 phosphorylation as well as total ErbB1 levels in the brain region surrounding the cerebroventricle of control rats. In contrast, the action of the ErbB1 inhibitors on the VHL model was less remarkable with the given basal reduction of ErbB signaling in this region. Although the present results controlled the pharmacological action of ErbB1 inhibitors, the antipsychotic mechanism of these inhibitors in the VHL model remains to be explored.

The three distinct quinazoline compounds, PD153035, ZD1839, and OSI-774, inhibit ErbB1 tyrosine kinase activity and are used for the treatment of lung cancer (33). As these compounds produce a variety of side effects in oncotherapy, we needed to consider the specificity and side effects of these compounds in this study. For instance, the calculated daily doses of these compounds in the present protocol were 4 – 40 μg/kg body weight per day. These doses are markedly lower than those given to human cancer patients, who receive 1 – 10 mg/kg body weight per day (45 – 47). In addition, we administered these compounds directly into the cerebroventricle of the brain and yet did not find any apparent changes in locomotor activity and tone-dependent learning in the rats receiving these inhibitors. ZD1839, but not PD153035 or OSI-774, showed an influence on startle amplitudes of control rats. Thus, adverse effects of these inhibitors

appeared to be limited in the present experimental paradigms.

We also needed to consider the molecular specificity of these compounds because quinazoline compounds can act on other types of tyrosine kinases such as platelet-derived growth factor (PDGF) receptors, and vascular endothelial growth factor (VEGF) receptors as well (48, 49). Nonetheless, in vitro kination assay revealed that ZD1839 has the highest specificity for the ErbB1 receptor. The half receptor binding constant (IC_{50}) of ZD1839 is 23 nM for ErbB1 and 3700 nM for ErbB2 (50). OSI-774 also shows relatively higher affinity for the ErbB1 receptor (51), and finally, PD153035 has the affinity for ErbB1 (25 pM in IC_{50}) but is also active with ErbB2 – 4 (52, 53). In light of these pharmaceutical data, we assume that the EGF receptor (ErbB1) is the primary molecular target of these compounds.

Recently, we found that subchronic oral administration of emodin (3-methyl-1,6,8-trihydroxyanthraquinone) suppresses acoustic higher pulse-alone responses and abolishes PPI deficits of rats treated with EGF as neonates. Because emodin is potent at inhibiting various tyrosine kinases including ErbB1 and ErbB2, the effect of emodin on PPI is in agreement with the present results obtained with the quinazoline derivatives. A difference between the effects of emodin and the quinazoline ErbB1 inhibitors is seen in the acoustic startle test: The quinazoline ErbB1 inhibitors elevated PPI levels of the VHL rats without affecting their startle amplitudes, but emodin influences both PPI levels and pulse-alone startle amplitudes. In this context, this specificity of the drug action supports the argument that the higher startle responses of VHL rats are distinct from their lower PPI levels.

Subchronic treatment with lower doses of clozapine or risperidone significantly ameliorates the PPI deficits of the VHL model (54). Similarly, acute administration of risperidone, clozapine, and olanzapine, but not haloperidol, is also able to reverse PPI deficits of this model (55). Such atypical antipsychotics are known to normalize abnormalities in latent inhibition as well (56), which is similar to the effects of ZD1839 in the present study. However, Rueter et al. indicate ineffectiveness of clozapine on social interaction deficits of the VHL model (54). Our preliminary study also found the ineffectiveness of the ErbB1 inhibitors in social interaction deficits of an EGF-induced schizophrenia model (ref. 10; M. Mizuno, unpublished data). In this context, the neurobehavioral action of the quinazoline ErbB1 inhibitors might resemble that of atypical antipsychotics. Because one of the pharmacological features of the antipsychotics is dopamine D2R–receptor antagonism (57), the reports that receptor blockade of D2R also attenuates ErbB1 signaling in the nervous system are noteworthy (58 – 60). In this context, the interactions between ErbB1 signaling and dopamine neurotransmission might be implicated in schizophrenia-related behavioral deficits. As we failed to find any pathological increase in ErbB1 signaling in the VHL model, the neural targets of ErbB1 inhibitors remain to be identified. It is possible that these inhibitors might indirectly modulate the neural activity associated with the behavioral deficits.

In conclusion, the ErbB1 inhibitors carrying quinazoline structures exerted anti-psychotic-like actions on an animal model for schizophrenia. In any case, the results from ErbB inhibitors warrant further investigation in other animal models for schizophrenia or even in patients with this illness. We hope that the present findings will facilitate the development of novel antipsychotic drugs targeting ErbB receptors.

Acknowledgments

We are grateful to Dr. B.K. Lipska for kind technical guidance. This study was supported by a grant-in-aid from the Health and Labor Sciences Research Grants, Core Research for Evolutional Science and Technology from the JST Corporation, and a grant for Promotion of Niigata University Research Projects. Preliminary parts of this study are filed as a patent application (USPTO, #20060167026).

References

1 Nawa H, Takahashi M, Patterson PH. Cytokine and growth factor involvement in schizophrenia – support for the developmental model. Mol Psychiatry. 2000;5:594–603.
2 Lang UE, Jockers-Scherübl MC, Hellweg R. State of the art of the neurotrophin hypothesis in psychiatric disorders: implications and limitations. J Neural Transm. 2004;111:387–411.
3 Bauer S, Kerr BJ, Patterson PH. The neuropoietic cytokine family in development, plasticity, disease and injury. Nat Rev Neurosci. 2007;8:221–232.
4 Meyer U, Feldon J, Yee BK. A review of the fetal brain cytokine imbalance hypothesis of schizophrenia. Schizophr Bull. 2009;35: 959–972.
5 Futamura T, Toyooka K, Iritani S, Niizato K, Nakamura R, Tsuchiya K, et al. Abnormal expression of epidermal growth factor and its receptor in the forebrain and serum of schizophrenic patients. Mol Psychiatry. 2002;7:673–682.
6 Ikeda Y, Yahata N, Ito I, Nagano M, Toyota T, Yoshikawa T, et al. Low serum levels of brain-derived neurotrophic factor and epidermal growth factor in patients with chronic schizophrenia. Schizophr Res. 2008;101:58–66.
7 Cohen BD, Green JM, Foy L, Fell HP. HER4-mediated biological and biochemical properties in NIH 3T3 cells. Evidence for HER1-HER4 heterodimers. J Biol Chem. 1996;271:4813–4818.
8 Mei L, Xiong WC. Neuregulin 1 in neural development, synaptic plasticity and schizophrenia. Nat Rev Neurosci. 2008;9:437–452.
9 Schneider MR, Wolf E. The epidermal growth factor receptor ligands at a glance. J Cell Physiol. 2009;218:460–466.
10 Futamura T, Kakita A, Tohmi M, Sotoyama H, Takahashi H,

Nawa H. Neonatal perturbation of neurotrophic signaling results in abnormal sensorimotor gating and social interaction in adults: implication for epidermal growth factor in cognitive development. Mol Psychiatry. 2003;8:19–29.

11 Mizuno M, Malta RS Jr, Nagano T, Nawa H. Conditioned place preference and locomotor sensitization after repeated administration of cocaine or methamphetamine in rats treated with epidermal growth factor during the neonatal period. Ann N Y Acad Sci. 2004;1025:612–618.

12 Tohmi M, Tsuda N, Mizuno M, Takei N, Frankland PW, Nawa H. Distinct influences of neonatal epidermal growth factor challenge on adult neurobehavioral traits in four mouse strains. Behav Genet. 2005;35:615–629.

13 Sotoyama H, Namba H, Takei N, Nawa H. Neonatal exposure to epidermal growth factor induces dopamine D2-like receptor supersensitivity in adult sensorimotor gating. Psychopharmacology (Berl). 2007;191:783–792.

14 Tsuda N, Mizuno M, Yamanaka T, Komurasaki T, Yoshimoto M, Nawa H. Common behavioral influences of the ErbB1 ligands transforming growth factor alpha and epiregulin administered to mouse neonates. Brain Dev. 2008;30:533–543.

15 Mizuno M, Kawamura H, Takei N, Nawa H. The anthraquinone derivative Emodin ameliorates neurobehavioral deficits of a rodent model for schizophrenia. J Neural Transm. 2008;115:521–530.

16 Lipska BK, Weinberger DR. To model a psychiatric disorder in animals: schizophrenia as a reality test. Neuropsychopharmacology. 2000;23:223–239.

17 Lipska BK. Using animal models to test a neurodevelopmental hypothesis of schizophrenia. J Psychiatry Neurosci. 2004;29: 282–286.

18 Lipska BK, Jaskiw GE, Weinberger DR. Postpubertal emergence of hyperresponsiveness to stress and to amphetamine after neonatal excitotoxic hippocampal damage: a potential animal model of schizophrenia. Neuropsychopharmacology. 1993;9:67–75.

19 Sams-Dodd F, Lipska BK, Weinberger DR. Neonatal lesions of the rat ventral hippocampus result in hyperlocomotion and deficits in social behaviour in adulthood. Psychopharmacology (Berl). 1997;132:303–310.

20 Al-Amin HA, Shannon Weickert C, Weinberger DR, Lipska BK. Delayed onset of enhanced MK-801-induced motor hyperactivity after neonatal lesions of the rat ventral hippocampus. Biol Psychiatry. 2001;49:528–539.

21 Swerdlow NR, Lipska BK, Weinberger DR, Braff DL, Jaskiw GE, Geyer MA. Increased sensitivity to the sensorimotor gating-disruptive effects of apomorphine after lesions of medial prefrontal cortex or ventral hippocampus in adult rats. Psychopharmacology (Berl). 1995;122:27–34.

22 Lipska BK, Swerdlow NR, Geyer MA, Jaskiw GE, Braff DL, Weinberger DR. Neonatal excitotoxic hippocampal damage in rats causes post-pubertal changes in prepulse inhibition of startle and its disruption by apomorphine. Psychopharmacology (Berl). 1995;122:35–43.

23 Chambers RA, Moore J, McEvoy JP, Levin ED. Cognitive effects of neonatal hippocampal lesions in a rat model of schizophrenia. Neuropsychopharmacology. 2001;15:587–594.

24 Grecksch G, Bernstein GH, Becker A, Hollt V, Bogerts B. Disruption of latent inhibition in rats with postnatal hippocampal lesions. Neuropsychopharmacology. 1999;20:525–532.

25 Lipska BK, Aultman JM, Verma A, Weinberger DR, Moghaddam B. Neonatal damage of the ventral hippocampus impairs working memory in the rat. Neuropsychopharmacology. 2002;27:47–54.

26 Levin ED, Christopher NC. Effects of clozapine on memory function in the rat neonatal hippocampal lesion model of schizophrenia. Prog Neuropsychopharmacol Biol Psychiatry. 2006;30: 223–229.

27 Richtand NM, Taylor B, Welge JA, Ahlbrand R, Ostrander MM, Burr J, et al. Risperidone pretreatment prevents elevated locomotor activity following neonatal hippocampal lesions. Neuropsychopharmacology. 2006;31:77–89.

28 Lipska BK, Lerman DN, Khaing ZZ, Weickert CS, Weinberger DR. Gene expression in dopamine and GABA systems in an animal model of schizophrenia: effects of antipsychotic drugs. Eur J Neurosci. 2003;18:391–402.

29 Nadri C, Lipska BK, Kozlovsky N, Weinberger DR, Belmaker RH, Agam G. Glycogen synthase kinase (GSK)-3beta levels and activity in a neurodevelopmental rat model of schizophrenia. Dev Brain Res. 2003;141:33–37.

30 Endo K, Hori T, Abe S, Asada T. Alterations in GABA(A) receptor expression in neonatal ventral hippocampal lesioned rats: comparison of prepubertal and postpubertal periods. Synapse. 2007;61:357–366.

31 Tseng KY, Chambers RA, Lipska BK. The neonatal ventral hippocampal lesion as a heuristic neurodevelopmental model of schizophrenia. Behav Brain Res. 2009;204:295–305.

32 Fry DW. Site-directed irreversible inhibitors of the erbB family of receptor tyrosine kinases as novel chemotherapeutic agents for cancer. Anticancer Drug Des. 2000;15:3–16.

33 Sridhar SS, Seymour L, Shepherd FA. Inhibitors of epidermal-growth-factor receptors: a review of clinical research with a focus on non-small-cell lung cancer. Lancet Oncol. 2003;4:397–406.

34 Mizuno M, Sotoyama H, Narita E, Kawamura H, Namba H, Zheng Y, et al. A cyclooxygenase-2 inhibitor ameliorates behavioral impairments induced by striatal administration of epidermal growth factor. J Neurosci. 2007;27:10116–10127.

35 Wang K, Kirichian AM, Aowad AF, Adelstein SJ, Kassis AI. Evaluation of chemical, physical, and biologic properties of tumor-targeting radioiodinated quinazolinone derivative. Bioconjug Chem. 2007;18:754–764.

36 Swerdlow NR, Braff DL, Geyer MA. Animal models of deficient sensorimotor gating: what we know, what we think we know, and what we hope to know soon. Behav Pharmacol. 2000;11:185–204.

37 Swerdlow NR, Geyer MA, Braff DL. Neural circuit regulation of prepulse inhibition of startle in the rat: current knowledge and future challenges. Psychopharmacology (Berl). 2001;156:194–215.

38 Arai S, Takuma K, Mizoguchi H, Ibi D, Nagai T, Takahashi K, et al. Involvement of pallidotegmental neurons in methamphetamine- and MK-801-induced impairment of prepulse inhibition of the acoustic startle reflex in mice: reversal by GABAB receptor agonist baclofen. Neuropsychopharmacology. 2008;33: 3164–3175.

39 Zhang WN, Murphy CA, Feldon J. Behavioural and cardiovascular responses during latent inhibition of conditioned fear: measurement by telemetry and conditioned freezing. Behav Brain Res. 2004;154:199–209.

40 McKillop D, Partridge EA, Kemp JV, Spence MP, Kendrew J, Barnett S, et al. Tumor penetration of gefitinib (Iressa), an epidermal growth factor receptor tyrosine kinase inhibitor. Mol

Cancer Ther. 2005;4:641–649.
41 Anttila S, Illi A, Kampman O, Mattila KM, Lehtimäki T, Leinonen E. Association of EGF polymorphism with schizophrenia in Finnish men. Neuroreport. 2004;15:1215–1218.
42 Stefansson H, Steinthorsdottir V, Thorgeirsson TE, Gulcher JR, Stefansson K. Neuregulin 1 and schizophrenia. Ann Med. 2004; 36:62–71.
43 Harrison PJ, Law AJ. Neuregulin 1 and schizophrenia: genetics, gene expression, and neurobiology. Biol Psychiatry. 2006;60: 132–140.
44 Nawa H, Takei N. Recent progress in animal modeling of immune inflammatory processes in schizophrenia: implication of specific cytokines. Neurosci Res. 2006;56:2–13.
45 Mei L, Xiong WC. Neuregulin 1 in neural development, synaptic plasticity and schizophrenia. Nat Rev Neurosci. 2008;9:437–452.
46 Herbst RS, Maddox AM, Rothenberg ML, Small EJ, Rubin EH, Baselga J, et al. Selective oral epidermal growth factor receptor tyrosine kinase inhibitor ZD1839 is generally well-tolerated and has activity in non-small-cell lung cancer and other solid tumors: results of a phase I trial. J Clin Oncol. 2002;20:3815–3825.
47 Pérez-Soler R, Chachoua A, Hammond LA, Rowinsky EK, Huberman M, Karp D, et al. Determinants of tumor response and survival with erlotinib in patients with non–small-cell lung cancer. J Clin Oncol. 2004;22:3238–3247.
48 Hennequin LF, Thomas AP, Johnstone C, Stokes ES, Plé PA, Lohmann JJ, et al. Design and structure-activity relationship of a new class of potent VEGF receptor tyrosine kinase inhibitors. J Med Chem. 1999;42:5369–5389.
49 Matsuno K, Ichimura M, Nakajima T, Tahara K, Fujiwara S, Kase H, et al. Potent and selective inhibitors of platelet-derived growth factor receptor phosphorylation. 1. Synthesis, structure-activity relationship, and biological effects of a new class of quinazoline derivatives. J Med Chem. 2002;45: 3057–3066.
50 Moulder SL, Yakes FM, Muthuswamy SK, Bianco R, Simpson JF, Arteaga CL. Epidermal growth factor receptor (HER1) tyrosine kinase inhibitor ZD1839 (Iressa) inhibits HER2/neu (erbB2)-overexpressing breast cancer cells in vitro and in vivo. Cancer Res. 2001;61:8887–8895.
51 Kim TE, Murren JR. Erlotinib OSI/Roche/Genentech. Curr Opin Investig Drugs. 2002;3:1385–1395.
52 Bridges AJ, Zhou H, Cody DR, Rewcastle GW, McMichael A, Showalter HD, et al. Tyrosine kinase inhibitors. 8. An unusually steep structure-activity relationship for analogues of 4-(3-bromoanilino)-6,7-dimethoxyquinazoline (PD 153035), a potent inhibitor of the epidermal growth factor receptor. J Med Chem. 1996;39:267–276.
53 Egeblad M, Mortensen OH, van Kempen LC, Jäättelä M. BIBX1382BS, but not AG1478 or PD153035, inhibits the ErbB kinases at different concentrations in intact cells. Biochem Biophys Res Commun. 2001;281:25–31.
54 Rueter LE, Ballard ME, Gallagher KB, Basso AM, Curzon P, Kohlhaas KL. Chronic low dose risperidone and clozapine alleviate positive but not negative symptoms in the rat neonatal ventral hippocampal lesion model of schizophrenia. Psychopharmacology (Berl). 2004;176:312–319.
55 Le Pen G, Moreau JL. Disruption of prepulse inhibition of startle reflex in a neurodevelopmental model of schizophrenia: reversal by clozapine, olanzapine and risperidone but not by haloperidol. Neuropsychopharmacology. 2002;27:1–11.
56 Weiner I, Feldon J. The latent inhibition model of schizophrenic attention disorder and of antipsychotic drug action. Psychopharmacology (Berl). 1994;116:379–381.
57 Meltzer HY, Matsubara S, Lee JC. Classification of typical and atypical antipsychotic drugs on the basis of dopamine D-1, D-2 and serotonin2 pKi values. J Pharmacol Exp Ther. 1989;251: 238–246.
58 Nair VD, Sealfon SC. Agonist-specific transactivation of phosphoinositide 3-kinase signaling pathway mediated by the dopamine D2 receptor. J Biol Chem. 2003;278:47053–47061.
59 Beom S, Cheong D, Torres G, Caron MG, Kim KM. Comparative studies of molecular mechanisms of dopamine D2 and D3 receptors for the activation of extracellular signal-regulated kinase. J Biol Chem. 2004;279:28304–28314.
60 O'Keeffe GC, Tyers P, Aarsland D, Dalley JW, Barker RA, Caldwell MA. Dopamine-induced proliferation of adult neural precursor cells in the mammalian subventricular zone is mediated through EGF. Proc Natl Acad Sci U S A. 2009;106:8754–8759.

Pharmacology, Biochemistry and Behavior 97 (2010) 392–398

Contents lists available at ScienceDirect

Pharmacology, Biochemistry and Behavior

journal homepage: www.elsevier.com/locate/pharmbiochembeh

The anthraquinone derivative emodin attenuates methamphetamine-induced hyperlocomotion and startle response in rats

Makoto Mizuno [a,*,1], Hiroki Kawamura [b,1], Yuta Ishizuka [b], Hidekazu Sotoyama [b], Hiroyuki Nawa [a,b]

[a] Center for Transdisciplinary Research, Niigata University, Niigata, Japan
[b] Department of Molecular Neurobiology, Brain Research Institute, Niigata University, Niigata, Japan

ARTICLE INFO

Article history:
Received 28 December 2009
Received in revised form 14 September 2010
Accepted 14 September 2010
Available online 21 September 2010

Keywords:
Anti-psychotic
Anthraquinone
Hypericin
Serotonin
Schizophrenia

ABSTRACT

Abnormal signaling mediated by epidermal growth factor (EGF) or its receptor (ErbB) is implicated in the neuropathology of schizophrenia. Previously, we found that the anthraquinone derivative emodin (3-methyl-1,6,8-trihydroxyanthraquinone) inhibits ErbB1 signaling and ameliorates behavioral deficits of the schizophrenia animal model established by EGF challenge. In the present study, we assessed acute and subchronic effects of its administration on methamphetamine-triggered behavioral hyperactivation in rats. Prior subchronic administration of emodin (50 mg/kg/day, 5 days, *p.o.*) suppressed both higher acoustic startle responses and hyperlocomotion induced by acute methamphetamine challenge. In parallel, emodin also attenuated methamphetamine-induced increases in dopamine and its metabolites and decreases in serotonin and its metabolites. Emodin administered alone also had an effect on stereotypic movement but no influence on horizontal or vertical locomotor activity. In contrast to pre-treatment, post-treatment with emodin had no effect on behavioral sensitization to methamphetamine. Administration of emodin in parallel to or following repeated methamphetamine challenge failed to affect hyperlocomotion induced by methamphetamine re-challenges. These findings suggest that emodin has unique pharmacological activity, which interferes with acute methamphetamine signaling and behavior.

1. Introduction

Emodin (3-methyl-1,6,8-trihydroxyanthraquinone) is extracted and purified from rhubarb. This natural compound has been proposed to attenuate signal transduction of growth factors and cytokines, inhibiting ErbB2, src-family kinase, IkappaB kinase, and extracellular signal-regulated kinase (ERK) (Jayasuriya et al., 1992; Kaneshiro et al., 2006; Kumar et al., 1998; Li et al., 2005; Wang et al., 2007b; Zhang et al., 1999). Recent pharmacological studies indicate that the influence of this compound on the brain and on behavioral traits (Gu et al., 2005; Lu et al., 2007). Our latest study suggests that emodin has anti-psychotic activity in a schizophrenia model established by neonatal epidermal growth factor (EGF) challenge (Mizuno et al., 2008), although it is unknown whether this anti-psychotic activity can be generalized for other animal models of psychosis.

In humans, chronic use of methamphetamine (MAP) causes drug addiction/relapse and evokes psychiatric symptoms such as hallucination and delusions, which are indistinguishable from paranoid schizophrenia (Kalechstein et al., 2003; Nordahl et al., 2002). In rodents, repeated exposure to MAP results in a progressive and long-lasting facilitation of the locomotor response, namely behavioral sensitization, which is often used as a model for drug addiction or relapse (Robinson and Berridge, 1993). The neural mechanism underlying induction and expression of behavioral sensitization involves a complex interplay among various neurotransmitters (Pierce and Kalivas, 1997; Vanderschuren and Kalivas, 2000) and cytokines (Flores et al., 2000; Horger et al., 1999; Messer et al., 2000; Mizuno et al., 2004; Nakajima et al., 2004; Pierce et al., 1999). Several lines of evidence indicate involvement of the ERK pathway in the integration of extracellular signals and in the long-term effects of MAP abuse (Mizoguchi et al., 2004; Valjent et al., 2006). MAP-induced behavioral impairment in rodents may be useful as an animal model for psychosis as well as for schizophrenia.

In the present study, we investigated acute and subchronic effects of emodin on MAP-induced hyperlocomotion and/or sensitization using MAP-challenged rats as a model for psychosis (Niwa et al., 2008). As emodin influences ErbB1/2 signaling and the ERK cascade, we monitored the phosphorylation states of these kinases in the

* Corresponding author. Center for Transdisciplinary Research, Brain Research Institute, Niigata University, 1-757 Asahimachi, Niigata 951-8585, Japan. Tel.: +81 25 227 0615; fax: +81 25 227 0815.
E-mail address: mizuno@bri.niigata-u.ac.jp (M. Mizuno).
[1] MM and HK contributed to this work equally.

0091-3057/$ – see front matter © 2010 Elsevier Inc. All rights reserved.
doi:10.1016/j.pbb.2010.09.009

brain. Bearing in mind the potential therapeutic applications, we orally administered emodin prior to, in conjunction with, or following MAP challenge to assess the potential pharmaceutical application of emodin for MAP psychosis.

2. Materials and methods

2.1. Animals

Sprague–Dawley rats (7–8 weeks postnatal, all male) were purchased from SLC Co., LTD (Shizuoka, Japan) and were maintained in a regulated environment (23 ± 1 °C) under a 12-h light–dark cycle (7:00 on −19:00 off) with free access to food and water. All of the animal experiments described here were performed in accordance with the Animal Use and Care Committee guidelines of Niigata University and the Guiding Principles for the Care and Use of Laboratory Animals approved by the Japanese Pharmacological Society.

2.2. Drug treatment

Emodin (>98% pure; Tokyo Chemical Industry Inc., Tokyo, Japan) was sonicated in a 10% lecithin solution (Wako Chemical Co., Osaka, Japan) at a concentration of 5 mg/ml. This emulsion of emodin (50 mg/kg) or vehicle (10% lecithin) was administered to rats with the aid of an oral zonde for rats (Natume Seisakusho Co., LTD, Japan), before or after MAP challenge. The given dose was optimized in our previous study (Mizuno et al., 2008) and set below the toxic amount of emodin (<80 mg/kg) reported by Jahnke et al. (2004). MAP was obtained as methamphetamine hydrochloride from Dainippon Pharmaceutical (Osaka, Japan) and dissolved in saline (1 mg/ml). In the paradigm (*A*) of the pre-treatment schedule, rats were given vehicle or emodin (*p.o.*) once daily for 5 days and then given MAP (1.0 mg/kg, *i.p.*) on day 6 (*A1*). To monitor the acute effect of emodin, alternatively, rats were subjected to another paradigm (*A2*): Rats were given emodin once and, 3 h later, were challenged with MAP (1.0 mg/kg). In the paradigm (*B*) of the co-treatment schedule, rats were given vehicle or emodin once daily for 5 days, then given vehicle plus MAP or emodin plus MAP for the following 5 days, and were finally challenged with MAP alone (1.0 mg/kg) on day 11. In the paradigm (*C*) of the post-treatment schedule, rats were given MAP (1.0 mg/kg) once daily for 7 days, then treated with vehicle or emodin daily for the following 7 days, and then challenged with MAP (1.0 mg/kg) on day 15. In paradigms (*A1*), (*B*) and (*C*), MAP challenge was performed more than 20 h after the last emodin treatment to minimize the acute effects of emodin.

2.3. Immunoblot analysis

Polyacrylamide gel electrophoresis (PAGE) and immunoblotting were performed as described previously (Mizuno et al., 2007). Cells were harvested, lysed, and sonicated in sample buffer (2% sodium dodecyl sulfate (SDS), 10 mM Tris–HCl, 150 mM NaCl, 2% SDS, 1 mM NaF, and 1 mM Na_3VO_4). After centrifugation, the supernatant was collected and the protein concentrations were determined. Equal amounts of protein were subjected to SDS-PAGE and transferred to PVDF membranes. Membranes were probed with anti-phosphorylated-ERK1/2 and anti-ERK1/2 (1:1000, Cell Signaling Tech, Danvers, MA, USA) and anti-β-actin antibodies (1:10,000, Chemicon Int, Temecula, CA, USA), followed by horseradish-peroxidase-conjugated anti-mouse IgG or horseradish-peroxidase-conjugated anti-rabbit IgG secondary antibodies (1:10,000, DAKO Cytomation, Glostrup, Denmark). Peroxidase activity was visualized by chemiluminescence (Western Lightning, Perkin Elmer, Tokyo, Japan) coupled with film exposure.

2.4. Quantification of monoamines and their metabolites

The assay for dopamine (DA), 3,4-dihydroxyphenylacetic acid (DOPAC), homovanillic acid (HVA), serotonin (5-HT), and 5-hydroxyindoleacetic acid (5-HIAA) is previously described (Futamura et al., 2003). One hour after MAP challenge, the striatum and frontal cortex were dissected and frozen on dry ice. The tissue samples were then weighed individually and stored at -80 °C. The samples were placed in 0.1 M perchloric acid containing isoproterenol (an internal standard). After sonication, the samples were vortexed and stored at 4 °C for 30 min. The samples were then centrifuged and the supernatant analyzed by high performance liquid chromatography with electrochemical detection (HPLC-ECD). The HPLC-ECD system consisted of a pump (model EP-10; EICOM, Kyoto, Japan) connected to an ODS column (model MA-5ODS; EICOM, 4.6×150 mm). Samples were separated with a mobile phase of 45 mM citric acid–50 mM sodium acetate buffer (pH 3.65), 285 mg/L octanesulfonic acid sodium salt, 0.13 mM EDTA, and 13% (v/v) methanol. Detection was performed electrochemically on a thin-layer cell with a glassy carbon-working electrode (model ECD-300; EICOM).

2.5. Measurement of acoustic startle responses

One hour after the last MAP challenge, acoustic startle responses were measured in a startle chamber (SR-Lab Systems, San Diego Instruments, San Diego, CA, USA) adapted for rats (Swerdlow and Geyer, 1998; Swerdlow et al., 2001). This paradigm was used to assess startle amplitude response with acoustic stimuli of 120 dB and background noise (white noise, 70 dB). Each rat was placed in the startle chamber and initially acclimatized for 5 min with background noise alone. The rats were then subjected to 16 trials, each trial repeated 8 times in a pseudorandom order: (i) a 40-ms 120-dB noise burst presented alone, or (ii) no stimulus (background noise alone). The inter-trial interval was 15 s. Analysis of acoustic startle response was based on the mean of eight trials.

2.6. Locomotor activity

We measured basal and MAP-induced locomotor activities of rats (120 min) in the afternoon. Locomotor activity was monitored before (60 min) and/or after MAP challenge (60 min) in a novel environment (Futamura et al., 2003; Mizuno et al., 2008). Each rat was placed in an open field box (45 cm length×45 cm width×30 cm height, MED Associates, St. Albans, VA, USA) under a moderate light level (400 Lx). Photo-beam sensors were used to measure line crossings and rearing counts (25-mm intervals for horizontal axis and 150-mm intervals for vertical axis).

2.7. Statistical analysis

Results are expressed as the means ± SEM. Behavioral data were analyzed by analysis of variance (ANOVA). When univariate data were obtained only from two groups, a two-tailed *t*-test was used for comparison. Locomotor scores were analyzed separately before and after MAP challenge using multiple repeated ANOVA with emodin administration (two levels) as between-subject factors, and time session for locomotor test (12 sessions) as a within-subject factor. Interaction of a within-subject factor with between-subject factors was estimated by MANOVA with Pilli tracing. Subsequently, a Fisher's LSD test was applied to absolute behavioral values as a *post-hoc* test of multiple comparisons. Alternatively, we performed the Student–Newman–Keuls multiple range test on multiple monoamine values to avoid type 2 error. A P value of less than 0.05 was regarded as statistically significant. Statistical analysis was performed using the SPSS software (version 11.5). N values in parentheses represent the number of animals used.

3. Results

3.1. Subchronic pre-treatment with emodin suppresses MAP-induced hyperlocomotion

To examine whether subchronic pre-treatment with emodin influences the effect of MAP on locomotor activity, rats that had previously been treated with various doses of emodin (0–50 mg/kg, *p.o.*) for 5 days were challenged with MAP (1.0 mg/kg, *i.p.*) (*Paradigm A1*). Rats were subjected to the locomotion test 1 h before MAP challenge. Subchronic pre-treatment with emodin reduced MAP-induced hyperlocomotion in a dose-dependent manner (60 min total: $F(3,16)=3.27$, $p=0.049$ by one-way ANOVA) (Fig. 1). *Post-hoc* analysis revealed that 20 and 50 mg/kg/day of emodin were sufficient to suppress MAP-induced hyperlocomotion. Accordingly, we used an emodin dose of 50 mg/kg/day for further studies.

Using a larger number of animals, we ascertained the effect of emodin on basal locomotor activity as well as on MAP-induced activity (Fig. 2). Subchronic pre-treatment with emodin alone (50 mg/kg/day, 5 days) did not influence basal horizontal locomotor activity in the novel environment (emodin, $F(1,13)=0.446$, $p=0.511$; time, $F(11,13)=10.1$, $p<0.001$; interaction of emodin and time, $F(11,13)=0.853$, $p=0.599$). Vertical movement (rearing) and ambulation scores were also indistinguishable between the emodin-pre-treated group and vehicle-pre-treated group: (emodin, $F(1,13)=2.10$, $p=0.161$; time, $F(11,13)=6.63$, $p=0.001$; interaction of emodin and time, $F(11,13)=1.68$, $p=0.185$). In contrast, emodin-pre-treatment significantly decreased stereotypic counts (emodin, $F(1,13)=5.80$, $p=0.024$; time, $F(11,13)=9.1$, $p<0.001$; interaction of emodin and time, $F(11,13)=2.88$, $p=0.037$).

Following 60 min of activity monitoring, we administered MAP to emodin- or vehicle-pre-treated rats (Fig. 2). MAP administration evoked hyperlocomotion in both groups but the magnitude of the behavioral enhancement was significantly lower in the emodin-pre-treated animals (emodin, $F(1,13)=12.27$, $p=0.002$; time, $F(11,13)=5.02$, $p=0.004$; interaction of emodin and time, $F(11,13)=2.06$, $p=0.108$). In parallel, emodin pre-treatment significantly attenuated vertical movement (emodin, $F(1,13)=4.91$, $p=0.037$; time, $F(11,13)=3.84$, $p=0.012$; interaction of emodin and time, $F(11,13)=2.07$, $p=0.107$) and ambulation scores (emodin, $F(1,13)=7.99$, $p=0.010$; time, $F(11,13)=3.77$, $p=0.013$; interaction of emodin and time, $F(11,13)=4.03$, $p=0.010$) induced by MAP. Stereotypic counts of emodin-pre-treated animals remained lower following MAP challenge (emodin, $F(1,13)=0.446$, $p=0.511$; time, $F(11,13)=9.1$, $p<0.001$; interaction of emodin and time, $F(11,13)=2.88$, $p=0.037$).

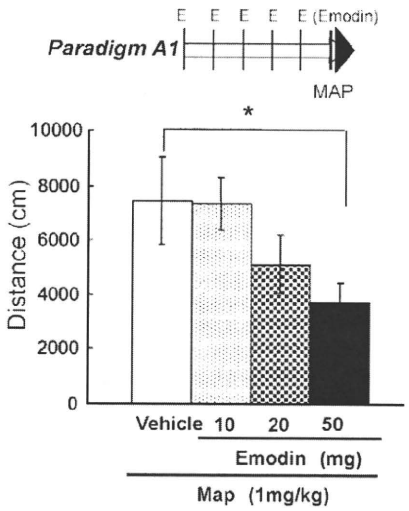

Fig. 1. Dose-dependent effects of emodin pre-treatment on MAP-induced hyperlocomotion in rats. Various doses of emodin (0, 10, 20, and 50 mg/kg weight) were orally administered to rats once a day for 5 days (i.e., days 1–5). Twenty to twenty-four hours after the final emodin treatment, MAP (1.0 mg/kg) was administered to the rats (*Paradigm A1*). Horizontal movement was monitored in a novel environment before and after MAP challenge. Bars indicate total distance of movement during the initial 60-min period (mean ± SE, $n=5$ each). *$p<0.05$ by ANOVA.

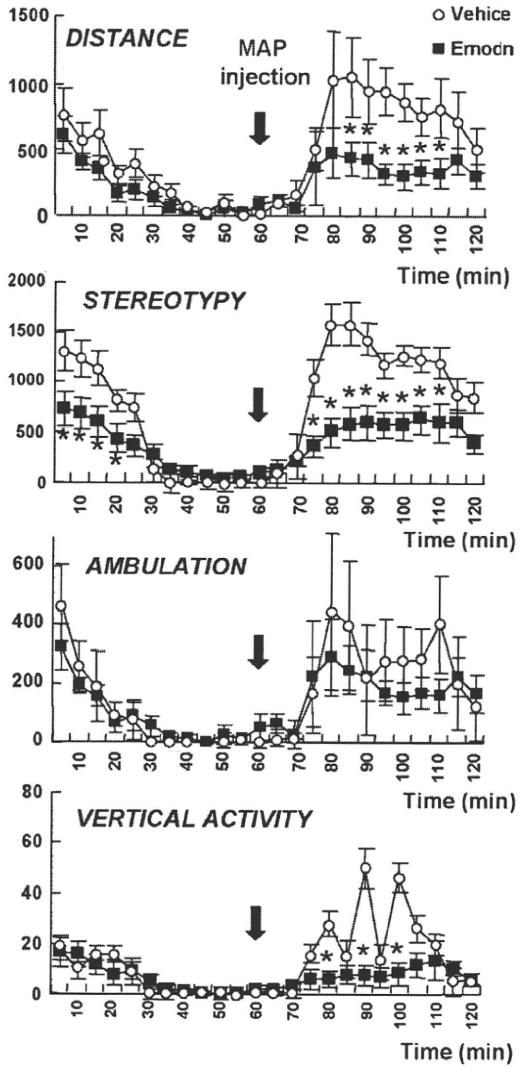

Fig. 2. Effects of subchronic pre-treatment with emodin on basal and MAP-induced locomotion in rats. Subchronic effects of emodin pre-treatment on distance (cm), ambulation (times), stereotypy (times), and vertical movement (times) of MAP-administered rats were examined with the experimental procedure detailed in Fig. 1 (*Paradigm A1*). Emodin was administered to rats once a day for 5 days (i.e., days 1–5). Twenty to twenty-four hours after the final emodin treatment, rats were subjected to an exploratory motor test before and after MAP challenge (1.0 mg/kg). Values indicate the mean ± SE ($n=7$–8). MAP-induced locomotion was compared between vehicle- and emodin-pre-treated groups by ANOVA, followed by *post-hoc*. *$p<0.05$ vs vehicle-treated group.

3.2. Subchronic pre-treatment with emodin suppresses MAP-induced acoustic startle responses

MAP elevates the magnitude of the acoustic startle response (Davis, 1988). To examine whether emodin affects MAP-induced acoustic startle response, rats were similarly treated with various doses of emodin (0–50 mg/kg, *p.o.*) for 5 days and then challenged with MAP as described above (*Paradigm A1*). As the initial dose of MAP (1.0 mg/kg, *i.p.*) failed to affect acoustic startle responses (data

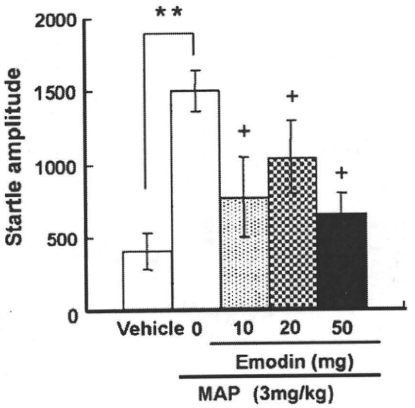

Fig. 3. Subchronic effects of emodin pre-treatment on MAP-induced hyperstartle responses. Various doses of emodin (10, 25, and 50 mg/kg/day) or vehicle were administered to rats once a day for 5 days (*Paradigm A1*). Twenty to twenty-four hours after the last emodin treatment, rats were challenged with MAP (3.0 mg/kg) and subjected to an acoustic startle test. Values indicate the mean ± SE (arbitrary unit; $n=5$ each). Startle responses to a 120 dB tone were compared among vehicle-treated and emodin-treated rats that were challenged with MAP. $^{**}p<0.01$ vs vehicle-treated group; $+p<0.05$ vs MAP-challenged naïve group.

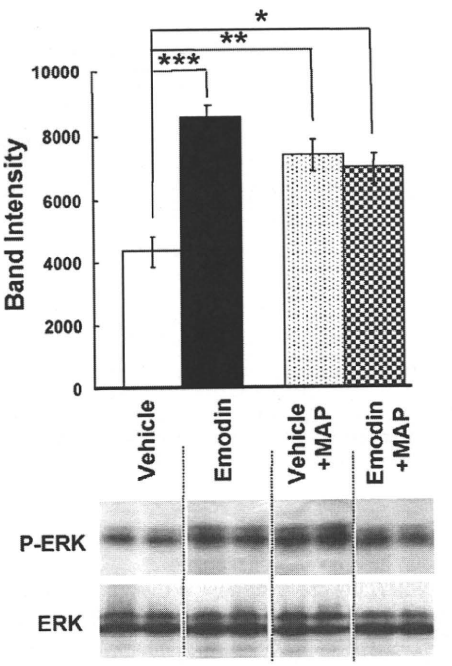

Fig. 4. Effect of emodin on phosphorylation of ERK1/2 in the striatum. Emodin or vehicle was administered to rats once a day for 5 days (days 1–5) (*Paradigm A1*). Rats were challenged with saline or MAP (1 mg/kg) on day 6 and killed 30 min after MAP challenge. Immunoblots of protein lysates from the whole striatum were probed with anti-phospho-ERK and anti-ERK antibodies. Values indicate the mean ± SE (arbitrary unit; $n=4$ each). Two representative lanes of immunoblots are displayed for each group. $^{*}p<0.05$. $^{**}p<0.01$, and $^{***}p<0.001$ vs the control group that was treated with vehicle but without MAP.

not shown), we increased the dose to 3.0 mg/kg (*i.p.*) and tested the startle responses to a 120-dB tone (Fig. 3). While acute administration of MAP significantly enhanced the startle responses, subchronic pre-treatment with emodin attenuated the MAP-induced hyperstartle response ($F(4,16)=8.13$, $p=0.005$ by one-way ANOVA). *Post-hoc* analysis revealed that an emodin dose of 10 mg/kg/day was sufficient to suppress MAP-induced acoustic hypersensitivity. In contrast to the above locomotion test results, the acoustic startle test did not display apparent emodin dose dependency.

3.3. Emodin alters ERK1/2 signaling, dopamine and serotonin metabolism

Emodin has been shown to attenuate growth factor signaling (Mizuno et al., 2008). MAP-induced behavioral impairment is associated with a disruption of extracellular receptor kinase1/2 (ERK1/2) signaling in the forebrain region (Kamei et al., 2006). To explore the contribution of ERK1/2 signaling, we examined the effects of emodin pre-treatment and after MAP challenge on ERK1/2 phosphorylation in the striatum of rats (Fig. 4). According to the above experimental protocol (*Paradigm A1*), rats were pre-treated with emodin or vehicle and then challenged with MAP (1 mg/kg) or saline. Consistent with previous studies, a significant increase in the level of phosphorylated ERK1/2 was observed following MAP challenge. Pre-treatment with emodin elevated basal phosphorylation of ERK1/2 and changed MAP-induced ERK expression and ERK phosphorylation ($F(1,12)=28.64$, $p<0.001$ for emodin, $F(1,12)=3.019$, $p=0.108$ for MAP but with an interaction; $F(1,12)=40.00$, $p<0.001$). However, the levels of total ERK1/2 did not differ among the groups examined ($F(1,12)=0.307$, $p=0.590$ for MAP and $F(1,12)=0.278$, $p=0.608$ for emodin without interaction $F(1,12)=0.024$, $p=0.880$).

Similarly, we monitored brain content of monoamine and its metabolites to assess the emodin effect on these neurotransmitters. Total monoamine was extracted from the frontal cortex and striatum of saline- and MAP-challenged rats that had been pre-treated with emodin or vehicle (Tables 1 and 2). We detected a significant increase in dopamine and its metabolites and a decrease in serotonin and its metabolites in both regions of the MAP-challenged rats. In contrast, subchronic treatment with emodin significantly attenuated MAP-induced increase in the content of dopamine and its metabolites in the striatum and also attenuated a MAP-induced decrease in the content of serotonin and its metabolites in the frontal cortex.

3.4. No effect of acute emodin treatment on MAP-induced hyperlocomotion

To examine whether acute intake of emodin affects MAP-induced hyperlocomotion, rats were given emodin once (50 mg/kg, *p.o.*) followed by MAP challenge (1.0 mg/kg, *i.p.*) with a 3-h delay (*Paradigm*

Table 1
Effects of emodin on dopamine metabolism in the frontal cortex and striatum.

Pre-treatment	Challenge	DA (pg/mg)	DOPAC (pg/mg)	HVA (pg/mg)
Frontal cortex				
Vehicle	SAL	4.20 ± 0.31a	1.15 ± 0.0,8a	1.30 ± 0.02a
Vehicle	MAP	5.75 ± 0.18a,b	2.53 ± 0.18a	1.52 ± 0.05a
Emodin	SAL	3.78 ± 0.31b	1.12 ± 0.10a	1.33 ± 0.02a
Emodin	MAP	5.45 ± 0.25a,b	2.26 ± 0.21a	1.89 ± 0.11a
Striatum				
Vehicle	SAL	364.29 ± 23.28a	46.19 ± 3.57a	5.81 ± 0.11a
Vehicle	MAP	417.68 ± 12.667a,b	90.89 ± 4.23a,b	12.69 ± 0.84a,b
Emodin	SAL	339.38 ± 10.37a,b	51.24 ± 6.94a,b	5.48 ± 0.60a,b
Emodin	MAP	366.77 ± 21.76b	72.80 ± 4.65b	11.07 ± 1.14b

Monoamines and their metabolites were extracted from frontal cortex and striatum 2 h after methamphetamine challenge (n = 6–7). Their concentrations were determined by HPLC-ECD. Abbreviations: DA; dopamine, DOPAC; 3,4-dihydroxyphenylacetic acid, HVA; homovanillic acid. Statistically homogeneous values are determined by the Student–Newman–Keuls multiple range test and marked with a or b.

Table 2
Effects of emodin on serotonin metabolism in the frontal cortex and striatum.

Pre-treatment	Challenge	5-HT (pg/mg)	5-HIAA (pg/mg)
Frontal cortex			
Vehicle	SAL	3.53 ± 0.28a	4.73 ± 0.79a
Vehicle	MAP	0.75 ± 0.11b	1.10 ± 0.08a
Emodin	SAL	1.58 ± 0.17b	2.90 ± 0.63a
Emodin	MAP	2.08 ± 0.11a,b	2.19 ± 0.08a
Striatum			
Vehicle	SAL	3.31 ± 0.28a	4.70 ± 0.27a
Vehicle	MAP	1.56 ± 0.17a,b	2.22 ± 0.13a,b
Emodin	SAL	1.61 ± 0.19a,b	2.33 ± 0.23a,b
Emodin	MAP	1.70 ± 0.16b	1.97 ± 0.16b

Monoamines and their metabolites were extracted from frontal cortex and striatum 2 h after methamphetamine challenge (n = 6–7). Their concentrations were determined by HPLC-ECD. Abbreviations: 5-HT; 5-hydroxytryptamine, 5-HIAA; 5-hydroxyindoleacetic acid. Statistically homogeneous values are determined by the Student–Newman–Keuls multiple range test and marked with a or b.

A2). One hour before MAP challenge, rats were subjected to the locomotion test. Acute pre-treatment with emodin had failed to alter MAP-induced hyperlocomotion (emodin, $F(1,14)=1.36$, $p=0.265$; time, $F(11,3)=17.82$, $p=0.018$; interaction of emodin and time, $F(11,3)=2.38$, $p=0.258$) (Fig. 5). MAP administration also failed to significantly alter other indices of ambulation, stereotypy and vertical movement (data not shown). Thus, acute treatment with emodin had no apparent action on MAP-induced hyperlocomotion.

3.5. Effects of parallel emodin treatment on MAP-induced behavioral sensitization

To examine whether emodin attenuates the establishment of MAP-induced behavioral sensitization, rats were pre-treated with emodin (50 mg/kg/day, *p.o.*) or saline for 5 days and then challenged with MAP (1.0 mg/kg/day, *i.p.*) with or without emodin (50 mg/kg/day, *p.o.*) for an additional 5 days. Parallel treatment with emodin failed to influence hyperlocomotion induced by the final MAP challenge (emodin, $F(1,13)=2.09$, $p=0.172$; time, $F(11,3)=2.45$, $p=0.250$; interaction of emodin and time, $F(11,3)=0.458$, $p=0.852$) (Fig. 6). Administration of emodin in parallel with MAP failed to significantly alter other indices of ambulation, stereotypy and vertical movement (data not shown).

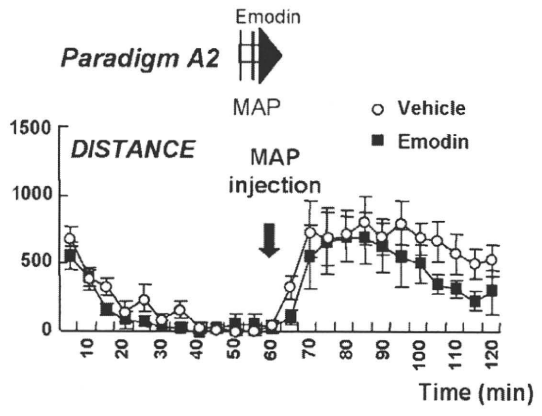

Fig. 5. Acute effect of emodin on MAP-induced hyperlocomotion. MAP-induced horizontal movement of rats was monitored 3 h after acute oral administration with emodin (50 mg/kg) (*Paradigm A2*). Values (cm) indicate the mean ± SE ($n=8$ each). MAP-induced locomotion was compared between vehicle- and emodin-pre-treated groups.

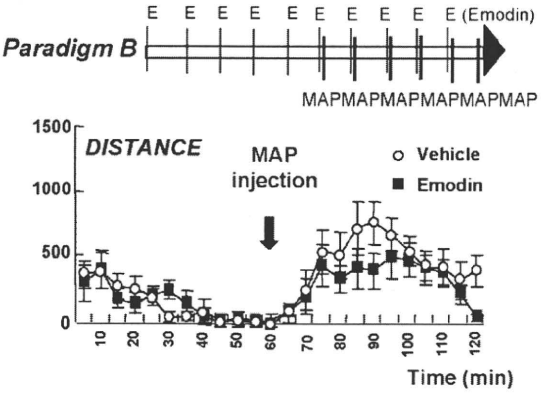

Fig. 6. Effect of parallel treatment with emodin and MAP. Emodin or vehicle was administered to rats once a day for 10 days (i.e., days 1–10). For the last 5 days, rats were additionally given MAP daily (1.0 mg/kg) (i.e., days 6–10). On day 11, all rats were re-challenged with MAP (1 mg/kg) to determine locomotor sensitization (*Paradigm B*). Locomotor activity (distance) was measured for 120 min before and after MAP treatment. Values (cm) indicate the mean ± SE ($n=7$–8).

3.6. Influence of emodin on maintenance of MAP-induced behavioral sensitization

To test the potential therapeutic applications of emodin, we investigated the effect of emodin treatment on behavioral sensitization established by repeated MAP pre-exposure and compared that with behavioral activation triggered by acute MAP challenge alone. Rats were pre-exposed to MAP treatment (1.0 mg/kg daily for 7 days) followed by emodin- or vehicle-treatment for 7 days (*Paradigm C*). Alternatively, another group of rats received emodin- or vehicle-treatment alone (*Paradigm A1*). Both groups were challenged with MAP and their horizontal activity was monitored for 15 min (Fig. 7). Two-way ANOVA with subject factors of MAP pre-exposure and emodin treatment revealed a significant main effect of MAP pre-exposure ($F(1,21)=24.9$, $p<0.001$) but not of emodin ($F(1,21)=0.202$, $p=0.658$) without an interaction of emodin and MAP pre-exposure ($F(1,21)<0.001$, $p=0.99$). This statistical result suggests that MAP pre-exposure established MAP sensitization in locomotor activity, but emodin treatment had no effect on MAP sensitization.

4. Discussion

The anthraquinone compound emodin, which is purified from natural herbal extracts, inhibits ErbB2-dependent cancer proliferation as well as several inflammatory signaling pathways (Jayasuriya et al., 1992; Kaneshiro et al., 2006; Kumar et al., 1998; Li et al., 2005; Wang et al., 2007b; Zhang et al., 1999). We previously found that emodin ameliorates EGF-induced behavioral deficits, inhibiting the activation of ErbB1 and ErbB2 (Mizuno et al., 2008). Subchronic oral administration of emodin (50 mg/kg/day) ameliorates behavioral abnormality in the acoustic startle reaction as well as in PPI without influencing locomotor activity or learning performance (Mizuno et al., 2008). Furthermore, we had evidence that emodin significantly reduced body weight 1 day after the first administration. However, from the third administration onwards there were similar positive weight gains in the emodin-treated group and the untreated group (Mizuno et al., 2008). As there were no significant effects from emodin administration, it seems less likely that the physical impact of emodin's laxative activity was causative for the effects of emodin on behavior. In the present study, this compound also impacts MAP-triggered behavioral abnormality. We found that repeated pre-treatment with emodin significantly attenuated hyperlocomotion triggered by MAP challenge, although parallel- and post-treatments with emodin failed to influence behavioral sensitization to MAP.

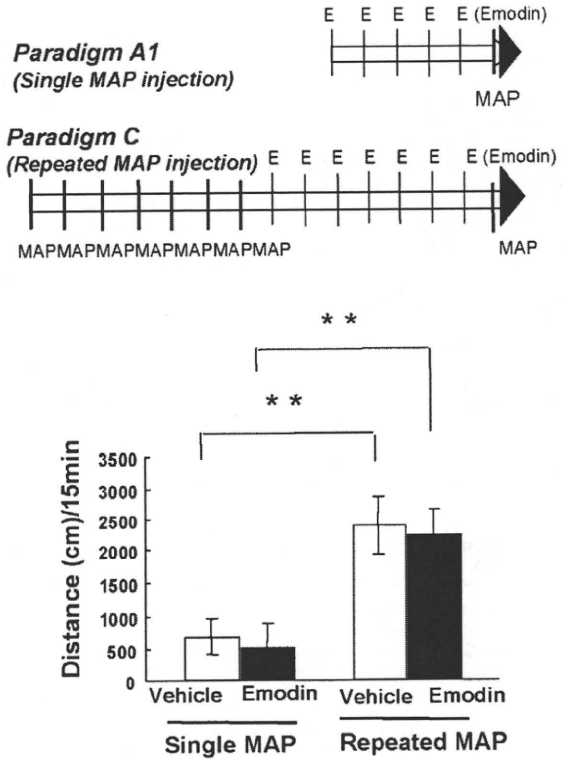

Fig. 7. Effect of emodin on the maintenance of MAP-induced sensitization in rats. Rats were challenged with MAP (1.0 mg/kg) daily for 7 days (i.e., days 1-7). For the next 7 days, rats were treated daily with emodin or vehicle (i.e., days 8–14). On day 15, all rats were re-challenged with MAP (1.0 mg/kg) (*Paradigm C*). In addition to *Paradigm C*, naïve rats were challenged with MAP in the presence or absence of emodin pre-treatment (*Paradigm A1*). Horizontal locomotor activity was also measured for 15 min after MAP challenge. Total distances were compared between acute and repeated MAP-injected groups or between emodin-treated and vehicle-treated group. Values indicate the mean ± SE ($n = 5$–8). $^{**}p<0.01$ by *post-hoc*.

These findings suggest that pre-treatment with emodin alone is capable of ameliorating the psychotic behaviors triggered by MAP. The effects of emodin on MAP-induced behaviors temporally contrast with those of neonatal EGF challenge. In the EGF model, emodin treatment is performed at the adult stage, which is preceded by neonatal behavioral sensitization with EGF, and is effective on adult behavioral impairment.

Emodin has been shown to suppress EGF receptor (ErbB1/2) activation (Mizuno et al., 2008; Zhang et al., 1999). Activation of tyrosine kinase receptors triggers multiple intracellular signaling pathways including ERK (Oda and Kitano, 2006). ERK1/2 signaling is implicated in the rewarding effects of MAP (Kamei et al., 2006; Mizoguchi et al., 2004) as well as in behavioral sensitization of cocaine (Valjent et al., 2004). Inhibition of ERK1/2 by microinjection of PD98059, an ERK1/2 kinase inhibitor, into the ventral striatum abolishes MAP-induced ERK1/2 activation and decreases the expression of MAP-induced conditioned place preference (Mizoguchi et al., 2004). Accordingly, we tested the hypothesis that suppression of ERK1/2 phosphorylation might underlie the emodin effects on MAP-induced behavior. In the present experiment, pre-treatment with emodin abolished the MAP-triggered increase in ERK phosphorylation; however, it up-regulated basal phosphorylation levels of ERK instead of decreasing them. In this context, we cannot rule out the possibility that the emodin-triggered increase in ERK phosphorylation in the striatum might be a secondary influence of emodin. Further studies are necessary to clarify the mechanism by which emodin modulates ERK1/2 activation and attenuates MAP-induced behavioral activation (Kaneshiro et al., 2006).

There are several natural anthraquinone derivatives such as emodin, sennoside, chrysophanol, aloe-emodin, physcion and rheum (Huang et al., 2007; Wang et al., 2001). Extracts from Chinese herbs containing these compounds are most famous for promoting defecation but may also possess additional activities, including the regulation of various psychiatric conditions. Previous studies on emodin pharmacology suggest that emodin decreases the release of the excitatory neurotransmitter glutamate in rat hippocampus (Gu et al., 2005) and also attenuates glutamate excitotoxicity of brain neurons (Wang et al., 2007a). In the present investigation, we found that subchronic emodin treatment attenuated an acute MAP-triggered increase in dopamine, DOPAC and HVA content, and decreased 5-HT and 5-HIAA content in both regions of the fontal cortex and striatum. This latter observation appears to agree with the findings that serotonin content is decreased after methamphetamine injections into the striatum (Fumagalli et al., 1998), the nucleus accumbens and caudate nucleus (Wallace et al., 1999), and the hippocampus (Rau et al., 2006). It is reported that serotonin release in the frontal cortex is increased by methamphetamine challenge (Ago et al., 2006, 2008). These results of serotonin release are different from our content data most likely because serotonin content indicates that serotonin storage may decrease after MAP-induced potentiation of serotonin efflux.

Emodin prevents cycloheximide-induced amnesia in rats. Emodin is also involved in the serotonergic roles on memory ameliorating effects (Lu et al., 2007). Another anthraquinone derivative, hypericin, is synthesized from emodin and has potent anti-depressant activity (Caccia, 2005). One of its pharmacological activities is the modulation of serotonin metabolism and release (Calapai et al., 2001a,b). Furthermore, in contemporary screening studies, hypericin has inhibitory effects on various pharmaceutically important enzymes such as MAO (monoaminoxidase), PKC (protein kinase C), dopamine-beta-hydroxylase, reverse transcriptase, telomerase, and CYP (cytochrome P450) (Kubin et al., 2005). Thus, hypericin has a pharmacological activity similar to emodin. These findings suggest that emodin and its derivatives have psychomodulatory activity and might alleviate the symptoms of psychiatric illness.

Acknowledgments

We would like to thank Ms. Chihiro Katsumoto for her technical assistance. This study was supported by: Health and Labor Sciences Research Grants (Research on Psychiatric and Neurological Diseases and Mental Health), Research Grants for Nervous and Mental Disorders from the Ministry of Health, Labor and Welfare, Core Research for Evolutional Science and Technology from the JST Corporation, and a grant for the Promotion of Niigata University Research Projects.

References

Ago Y, Nakamura S, Uda M, Kajii Y, Abe M, Bâaba A, et al. Attenuation by the 5-HT1A receptor agonist osemozotan of the behavioral effects of single and repeated methamphetamine in mice. Neuropharmacology 2006;51:914–22.

Ago Y, Nakamura S, Baba A, Matsuda T. Neuropsychotoxicity of abused drugs: effects of serotonin receptor ligands on methamphetamine- and cocaine-induced behavioral sensitization in mice. J Pharmacol Sci 2008;106:15–21.

Caccia S. Antidepressant-like components of Hypericum perforatum extracts: an overview of their pharmacokinetics and metabolism. Curr Drug Metab 2005;66: 531–43.

Calapai G, Crupi A, Firenzuoli F, Inferrera G, Squadrito F, Parisi A, et al. Serotonin, norepinephrine and dopamine involvement in the antidepressant action of hypericum perforatum. Pharmacopsychiatry 2001a;34:45–9.

Calapai G, Crupi A, Firenzuoli F, Inferrera G, Ciliberto G, Parisi A, et al. Interleukin-6 involvement in antidepressant action of Hypericum perforatum. Pharmacopsychiatry 2001b;34(Suppl 1):S8–10.

Davis M. Apomorphine, d-amphetamine, strychnine and yohimbine do not alter prepulse inhibition of the acoustic startle reflex. Psychopharmacology (Berl) 1988;95:151–6.

Flores C, Samaha AN, Stewart J. Requirement of endogenous basic fibroblast growth factor for sensitization to amphetamine. J Neurosci 2000;20:RC55.

Fumagalli F, Gainetdinov RR, Valenzano KJ, Caron MG. Role of dopamine transporter in methamphetamine-induced neurotoxicity: evidence from mice lacking the transporter. J Neurosci 1998;18:4861–9.
Futamura T, Kakita A, Tohmi M, Sotoyama H, Takahashi H, Nawa H. Neonatal perturbation of neurotrophic signaling results in abnormal sensorimotor gating and social interaction in adults: implication for epidermal growth factor in cognitive development. Mol Psychiatry 2003;8:19–29.
Gu JW, Hasuo H, Takeya M, Akasu T. Effects of emodin on synaptic transmission in rat hippocampal CA1 pyramidal neurons in vitro. Neuropharmacology 2005;49: 103–11.
Horger BA, Iyasere CA, Berhow MT, Messer CJ, Nestler EJ, Taylor JR. Enhancement of locomotor activity and conditioned reward to cocaine by brain-derived neurotrophic factor. J Neurosci 1999;19:4110–22.
Huang Q, Lu G, Shen HM, Chung MC, Ong CN. Anti-cancer properties of anthraquinones from rhubarb. Med Res Rev 2007;27:609–30.
Jahnke GD, Price CJ, Marr MC, Myers CB, George JD. Developmental toxicity evaluation of emodin in rats and mice. Birth Defects Res B Dev Reprod Toxicol 2004;71:89-101.
Jayasuriya H, Koonchanok NM, Geahlen RL, McLaughlin JL, Chang CJ. Emodin, a protein tyrosine kinase inhibitor from *Polygonum cuspidatum*. J Nat Prod 1992;55:696–8.
Kalechstein AD, Newton TF, Green M. Methamphetamine dependence is associated with neurocognitive impairment in the initial phases of abstinence. J Neuropsychiatry Clin Neurosci 2003;15:215–20.
Kamei H, Nagai T, Nakano H, Togan Y, Takayanagi M, Takahashi K, et al. Repeated methamphetamine treatment impairs recognition memory through a failure of novelty-induced ERK1/2 activation in the prefrontal cortex of mice. Biol Psychiatry 2006;59:75–84.
Kaneshiro T, Morioka T, Inamine M, Kinjo T, Arakaki J, Chiba I, et al. Anthraquinone derivative emodin inhibits tumor-associated angiogenesis through inhibition of extracellular signal-regulated kinase 1/2 phosphorylation. Eur J Pharmacol 2006;553:46–53.
Kubin A, Wierrani F, Burner U, Alth G, Grünberger W. Hypericin—the facts about a controversial agent. Curr Pharm Des 2005;11:233–53.
Kumar A, Dhawan S, Aggarwal BB. Emodin (3-methyl-1, 6, 8-trihydroxyanthraquinone) inhibits TNF-induced NF-kappaB activation, IkappaB degradation, and expression of cell surface adhesion proteins in human vascular endothelial cells. Oncogene 1998;17:913–8.
Li HL, Chen HL, Li H, Zhang KL, Chen XY, Wang XW, et al. Regulatory effects of emodin on NF-kappaB activation and inflammatory cytokine expression in RAW 264.7 macrophages. Int J Mol Med 2005;16:41–7.
Lu MC, Hsieh MT, Wu CR, Cheng HY, Hsieh CC, Lin YT, et al. Ameliorating effect of emodin, a constitute of *Polygonatum multiflorum*, on cycloheximide-induced impairment of memory consolidation in rats. J Ethnopharmacol 2007;112:552–6.
Messer CJ, Eisch AJ, Carlezon Jr WA, Whisler K, Shen L, Wolf DH, et al. Role for GDNF in biochemical and behavioral adaptations to drugs of abuse. Neuron 2000;26: 247–57.
Mizoguchi H, Yamada K, Mizuno M, Mizuno T, Nitta A, Noda Y, et al. Regulations of methamphetamine reward by extracellular signal-regulated kinase 1/2/ets-like gene-1 signaling pathway via the activation of dopamine receptors. Mol Pharmacol 2004;65:1293–301.
Mizuno M, Malta Jr RS, Nagano T, Nawa H. Conditioned place preference and locomotor sensitization after repeated administration of cocaine or methamphetamine in rats treated with epidermal growth factor during the neonatal period. Ann NY Acad Sci 2004;1025:612–8.
Mizuno M, Sotoyama H, Narita E, Kawamura H, Namba H, Zheng Y, et al. A cyclooxygenase-2 inhibitor ameliorates behavioral impairments induced by striatal administration of epidermal growth factor. J Neurosci 2007;27:10116–27.
Mizuno M, Kawamura H, Takei N, Nawa H. The anthraquinone derivative emodin ameliorates neurobehavioral deficits of a rodent model for schizophrenia. J Neural Transm 2008;115:521–30.
Nakajima A, Yamada K, Nagai T, Uchiyama T, Miyamoto Y, Mamiya T, et al. Role of tumor necrosis factor-alpha in methamphetamine-induced drug dependence and neurotoxicity. J Neurosci 2004;24:2212–25.
Niwa M, Yan Y, Nabeshima T. Genes and molecules that can potentiate or attenuate psychostimulant dependence: relevance of data from animal models to human addiction. Ann NY Acad Sci 2008;1141:76–95.
Nordahl TE, Salo R, Possin K, Gibson DR, Flynn N, Leamon M, et al. Low N-acetyl-aspartate and high choline in the anterior cingulum of recently abstinent methamphetamine-dependent subjects: a preliminary proton MRS study. Magnetic resonance spectroscopy. Psychiatry Res 2002;116:43–52.
Oda K, Kitano H. A comprehensive map of the toll-like receptor signaling network. Mol Syst Biol 2006;2 2006.0015.
Pierce RC, Kalivas PW. A circuitry model of the expression of behavioral sensitization to amphetamine-like psychostimulants. Brain Res Rev 1997;25:192–216.
Pierce RC, Pierce-Bancroft AF, Prasad BM. Neurotrophin-3 contributes to the initiation of behavioral sensitization to cocaine by activating the Ras/mitogen-activated protein kinase signal transduction cascade. J Neurosci 1999;19:8685–95.
Rau KS, Birdsall E, Volz TJ, Riordan JA, Baucum II AJ, Adair BP, et al. Methamphetamine administration reduces hippocampal vesicular monoamine transporter-2 uptake. J Pharmacol Exp Ther 2006;318:676–82.
Robinson TE, Berridge KC. The neural basis of drug craving: an incentive-sensitization theory of addiction. Brain Res Rev 1993;18:247–91.
Swerdlow NR, Geyer MA. Using an animal model of deficient sensorimotor gating to study the pathophysiology and new treatments of schizophrenia. Schizophr Bull 1998;24:285–301.
Swerdlow NR, Geyer MA, Braff DL. Neural circuit regulation of prepulse inhibition of startle in the rat: current knowledge and future challenges. Psychopharmacology (Berlin) 2001;156:194–215.
Valjent E, Pages C, Herve D, Girault JA, Caboche J. Addictive and non-addictive drugs induce distinct and specific patterns of ERK activation in mouse brain. Eur J Neurosci 2004;19:1826–36.
Valjent E, Corvol JC, Trzaskos JM, Girault JA, Hervé D. Role of the ERK pathway in psychostimulant-induced locomotor sensitization. BMC Neurosci 2006;7:20.
Vanderschuren LJ, Kalivas PW. Alterations in dopaminergic and glutamatergic transmission in the induction and expression of behavioral sensitization: a critical review of preclinical studies. Psychopharmacology (Berl) 2000;151:99-120.
Wallace TL, Gudelsky GA, Vorhees CV. Methamphetamine-induced neurotoxicity alters locomotor activity, stereotypic behavior, and stimulated dopamine release in the rat. J Neurosci 1999;19:9141–8.
Wang SC, Zhang L, Hortobagyi GN, Hung MC. Targeting HER2: recent developments and future directions for breast cancer patients. Semin Oncol 2001;Suppl 18:21–9.
Wang C, Zhang D, Ma H, Liu J. Neuroprotective effects of emodin-8-O-beta-D-glucoside in vivo and in vitro. Eur J Pharmacol 2007a;577:58–63.
Wang R, Wan Q, Zhang Y, Huang F, Yu K, Xu D, et al. Emodin suppresses interleukin-1beta induced mesangial cells proliferation and extracellular matrix production via inhibiting P38 MAPK. Life Sci 2007b;80:2481–8.
Zhang L, Lau YK, Xia W, Hortobagyi GN, Hung MC. Tyrosine kinase inhibitor emodin suppresses growth of HER-2/neu-overexpressing breast cancer cells in athymic mice and sensitizes these cells to the inhibitory effect of paclitaxel. Clin Cancer Res 1999;5:343–53.

J Neural Transm (2010) 117:887–895
DOI 10.1007/s00702-010-0418-3

BIOLOGICAL PSYCHIATRY - ORIGINAL ARTICLE

Measurement and comparison of serum neuregulin 1 immunoreactivity in control subjects and patients with schizophrenia: an influence of its genetic polymorphism

M. Shibuya · E. Komi · R. Wang · T. Kato · Y. Watanabe · M. Sakai · M. Ozaki · T. Someya · H. Nawa

Received: 17 February 2010 / Accepted: 2 May 2010 / Published online: 5 June 2010

Abstract *Neuregulin-1* (*NRG1*) gene is implicated in the etiology or neuropathology of schizophrenia, although its biological contribution to this illness is not fully understood. We have established an enzyme-linked immunosorbent assay (ELISA), which recognizes the NRG1β1 immunoglobulin-like (Ig) domain, and measured soluble Ig-NRG1 immunoreactivity in the sera of chronic schizophrenia patients ($n = 40$) and healthy volunteers ($n = 59$). ELISA detected remarkably high concentrations of Ig-NRG1 immunoreactivity in human serum (mean 5.97 ± 0.40 ng/mL, ~213 ± 14 pM). Gender and diagnosis exhibited significant effects on serum Ig-NRG1 immunoreactivity. Mean Ig-NRG1 immunoreactivity in the schizophrenia group was 63.2% of that measured in the control group. Ig-NRG1 immunoreactivity in women was 147.1% of that seen in men. We also attempted to correlate six SNPs of NRG1 genome with serum Ig-NRG1 immunoreactivity. Analysis of covariance with compensation for gender identified a significant interaction between diagnosis and SNP8NRG243177 allele. The T allele of this SNP significantly contributed to the disease-associated decrease in Ig-NRG1 immunoreactivity. Although we hypothesized a chronic influence of antipsychotic medications, there was no significant effect of chronic haloperidol treatment on serum Ig-NRG1 immunoreactivity in monkeys. These findings suggest that serum NRG1 levels are decreased in patients with chronic schizophrenia and influenced by their SNP8NRG243177 alleles.

Keywords Neuregulin · Schizophrenia · Serum · ELISA · SNP

Abbreviations

NRG	Neuregulin
SNP	Single-nucleotide polymorphism
ELISA	Enzyme-linked immunosorbent assay
LI	Like immunoreactivity
ANOVA	Analysis of variance
ANCOVA	Analysis of covariance

Introduction

Many studies have indicated a genetic linkage between the human chromosome locus 8p21-p12 and schizophrenia (Blouin et al. 1998; Kendler et al. 1996; Pulver et al. 1995). Stefansson et al. (2002) first reported that the *neuregulin-1* (*NRG1*) gene, which resides in this genomic locus, is associated with the vulnerability to schizophrenia. Subsequent studies have confirmed the genetic association with *NRG1* throughout different countries and populations

M. Shibuya · E. Komi · R. Wang · T. Kato · M. Sakai · H. Nawa (✉)
Department of Molecular Neurobiology, Brain Research Institute, Niigata University, 1-757, Asahimachi-dori, Niigata 951-8585, Japan
e-mail: hnawa@bri.niigata-u.ac.jp

M. Shibuya · Y. Watanabe · M. Sakai · T. Someya
Department of Psychiatry, Niigata University Graduate School of Medical and Dental Sciences, 1-757, Asahimachi-dori, Niigata 951-8510, Japan

M. Ozaki
Institute for Biomedical Engineering, Consolidated Research Institute for Advanced Science and Medical Care, Waseda University, 513, Wasedatsurumaki-cho, Shinjuku-ku, Tokyo 162-0041, Japan

(Addington et al. 2007; Corvin et al. 2004; Fukui et al. 2006; Gardner et al. 2006; Harrison and Weinberger 2005; Li et al. 2004; Tang et al. 2004; Thomson et al. 2007; Williams et al. 2003; Yang et al. 2003), although there are several contradictory reports (Ikeda et al. 2008; Iwata et al. 2004; Munafò et al. 2006; Thiselton et al. 2004). Postmortem studies support a genetic contribution of *NRG1* to schizophrenia (Hashimoto et al. 2004; Law et al. 2006). The expression of mRNAs encoding *NRG1* precursors is altered in schizophrenia patients; in particular, the type-I splice variants of *NRG1* mRNA are upregulated in the prefrontal cortex and hippocampus of affected patients (Hashimoto et al. 2004; Law et al. 2006). Although studies have attempted to correlate abnormalities in NRG1 mRNA expression with patient single nucleotide polymorphism (SNP) haplotype (Law et al. 2006), controversy surrounds the use of postmortem samples, especially for mRNA analysis (Chagnon et al. 2008; Harrison et al. 1995; Morrison-Bogorad et al. 1995; Tomita et al. 2004). Terminal conditions, such as coma and hypoxia, might influence *NRG1* gene expression and RNA quality in the brain (Chagnon et al. 2008; Harrison et al. 1995; Morrison-Bogorad et al. 1995; Tomita et al. 2004).

mRNA and protein measurements in blood are often used to diagnose schizophrenia or investigate the pathological contribution of individual molecules (Chagnon et al. 2008; Petryshen et al. 2005; Zhang et al. 2008). Of the molecules examined, growth factors and cytokines displayed marked abnormalities in both central nervous system and peripheral blood (Bellon 2007; Futamura et al. 2002; Sei et al. 2007; Takahashi et al. 2000; Toyooka et al. 2002, 2003). mRNA expression levels for *NRG1* precursors are determined by evaluation of peripheral lymphocytes from schizophrenia patients (Chagnon et al. 2008; Petryshen et al. 2005; Zhang et al. 2008). However, NRG1 peptide levels in peripheral blood have not yet been studied. The production and release of mature NRG1 peptides require proteolytic processing of precursors (i.e., ectodomain shedding) (Marchionni et al. 1993; Shirakabe et al. 2001; Yokozeki et al. 2007). This process liberates mature NRG1 peptides from the cell-anchored precursor proteins, allowing it to activate ErbB receptors. Thus, the measurement of free mature NRG1 peptides is necessary to estimate the biological activity.

Here, we established an enzyme-linked immunosorbent assay (ELISA) for NRG1 and measured trace NRG1-like immunoreactivities (LI) in the cell-free soluble fraction of human serum. ELISA allowed us to estimate the effects of gender, age and schizophrenia diagnosis, disease duration and antipsychotic treatment on human serum NRG1 peptide levels. We also attempted to estimate the contribution of SNPs in *NRG1* genome to serum NRG1-LI levels.

Materials and methods

Subjects

This clinical study was approved by the Ethics Committee on Genetics of the Niigata University School of Medicine. Written informed consent was obtained from all participants. Patients meeting the Diagnostic and Statistical Manual of Mental Disorders, fourth edition (DSM-IV) criteria for schizophrenia were recruited from two hospitals. The diagnosis of schizophrenia was based on all available sources of information, including unstructured interviews, clinical observations and medical records. Control subjects were recruited primarily from the staff of participating hospitals and associated laboratories. We matched the ages and genders of the control healthy volunteers to those of the patients examined. Although these subjects were not assessed by a structured psychiatric interview, all of them demonstrated good social and occupational skills and did not report any history of psychiatric disorders.

Three young adult male cynomolgus monkeys (*Macaca fascicularis*), 4 years of age, weighing 3.12–3.98 kg, were used in this study. Monkeys, reared at the animal house of Shinn Nippon Biomedical Lab. Inc. (Kagoshima, Japan), were housed individually in stainless steel cages of 50 cm (*W*) × 86 cm (*D*) × 82 cm (*H*) under temperature-controlled conditions, at 26 ± 2°C and a humidity of 40–60% under a 12/12-h light/dark cycle. Animals were fed 108 g commercial monkey chow daily. Filtered water was delivered by an automatic supplier ad libitum. Experiments were subjected to review by the Ethical Committee of Shinn Nippon Biomedical Lab. Inc., and were performed in accordance with the NIH Guidelines for the Care and Use of Laboratory Animals and the Guidelines of the Central Research Laboratory.

Blood sampling

Blood was collected in vacuum collection tubes (Neotube, NP-PS0507, Nipro, Osaka, Japan) between 9 and 12 a.m. in the morning. Within 1 h of collection, blood was coagulated at 37°C for 60 min. Serum was separated by centrifugation at 4°C for 15 min and stored at −80°C until use for analysis.

NRG enzyme immunoassay

We produced anti-NRG1β1 polyclonal antibodies by immunizing rabbits and guinea pigs with a mouse cerebellar isoform of NRG1β1 peptide (Ozaki et al. 2000). This type-I isoform, with a molecular weight of 25,500 Da,

consists of an immunoglobulin-like (Ig) domain and an epidermal growth factor (EGF)-like domain alone. Rabbit and guinea pig antisera were subjected to antigen-affinity chromatography (Affi-Gel 10, Bio-Rad, Hercules, CA, USA). We established ELISA using the affinity-purified antibodies according to the previous procedures (Nawa et al. 1995).

In brief, ELISA titer plates were coated with 100 ng rabbit anti-NRG1β1 antibody per well in 0.1 M Tris buffer (pH 9.0) for 12–18 h and then blocked with ELISA buffer [50 mM Tris, 0.5 M NaCl, 0.1% NaN_3, 0.2% Triton X-100, 1% gelatin (pH 6.8)] at 4°C for more than 12 h. Serum (100 μL; quadruplicate) or standard NRG1β3 (10–1,000 pg; quadruplicate) was loaded into wells. After five washes, each well was incubated with 30 ng of guinea pig anti-NRG1β1 antibody followed by rabbit anti-guinea pig Ig biotinylated antibody (1:5,000; Open Biosystems, Huntsville, AL, USA). Biotinylated antibodies bound to wells were incubated with 100 μL avidin-β-galactosidase (1:10,000; Rockland Immunochemicals Inc., Gilbertsville, PA, USA) followed by the fluorogenic substrate, 200 μM 4-methylumbelliferyl-β-D-galactoside (MUG; Sigma Chemicals, St. Louis, MO, USA). The fluorescent product was quantitated using an MTP-601F microplate reader (Corona, Ibaraki, Japan) with excitation and emission at 365 and 450 nm, respectively. To evaluate the cross-reactivity of ELISA, we obtained the following human recombinant factors that exhibit structural homology or similarity to NRG1: betacellulin, EGF, heparin-binding EGF-like growth factor (HB-EGF), epiregulin and transforming growth factor-α (TGFα) (Peprotech, Rocky Hill, NJ, USA, or Sigma Chemicals, St. Louis, MO, USA). The mature human NRG1β3 peptides, which correspond to the respective extracellular domains of NRG1 precursors (Genbank; NM_013956.3 for type I, NM_013962.2 for type II, and NM_013959.3 for type III), were synthesized by an in vitro translation/transcription system (T_NT Quick Coupled transcription/Translation Systems; Promega, Addison, WI, USA) using synthetic cDNAs encoding the corresponding domains (GenScript, Piscataway, NJ, USA). The amount of each type of NRG1β3 peptides was determined by immunoblotting for their histidine tag (R. Wang, unpublished data).

Genotyping

DNA was extracted from blood clots using Puregene core kit A (Qiagen, Germantown, MD, USA). We selected six SNPs from the human *NRG1* genome, which have been intensively characterized previously, to investigate rs35753505 (SNP8NRG221533), SNP8NRG241930, rs6994992 (SNP8NRG243177), rs1081062, rs3924999 and rs2954041 (Ikeda et al. 2008). These six SNPs were genotyped using the TaqMan assay as described previously (Fukui et al. 2006).

Chronic treatment of cynomolgus monkeys with haloperidol

Young adult monkeys (all male) were given oral haloperidol for 2 months. Haloperidol (Wako Chemical Ltd, Tokyo, Japan), suspended in 0.5% methylcellulose solution, was administered at concentrations of 0.125–0.25 mg/mL to monkeys daily with the aid of a gastric tube for 8 weeks. The initial dose of 0.25 mg/kg for 2 weeks was increased to 0.5 mg/kg for the following 6 weeks. We confirmed normal food consumption daily and monitored body weight gain weekly to avoid adverse effects of haloperidol treatment. Whole blood (5 mL/animal) was collected from the femoral vein before treatment and after 4 and 8 weeks of haloperidol treatment. Serum samples were prepared to measure haloperidol concentrations as well as Ig-NRG-LI levels.

Statistical analysis

To analyze multifactorial interactions and ascertain statistical power, we applied parametric analyses to data. Genotype deviation from Hardy–Weinberg equilibrium (HWE) and allele frequency difference between patients and controls were evaluated by using the χ^2 test. ELISA data were initially analyzed with the analysis of variance (ANOVA) using gender, disease, DSM-IV type and/or genotype as between-subject factors. The correlations between each potential confounding factor and Ig-NRG1-LI levels were examined by Pearson correlation analysis. The putative confounding factors included age, gender, duration of illness, age at onset and dose of antipsychotic medication. As we identified a significant and strong correlation of ELISA data with gender in the initial analysis, data were all re-analyzed using analysis of covariance (ANCOVA), adopting gender as a covariate. We used Fisher least significant difference (LSD) test for post hoc analysis. A probability level of $P < 0.05$ was considered to be statistically significant. All data represent the mean ± SE. Statistical analysis was performed using SPSS software (version 11.5).

Results

Establishment of a sandwich ELISA for NRG1

We raised antisera directed against recombinant mouse NRG1β1 (type I, soluble mature form) in rabbits and guinea pigs and established a sandwich ELISA for NRG1

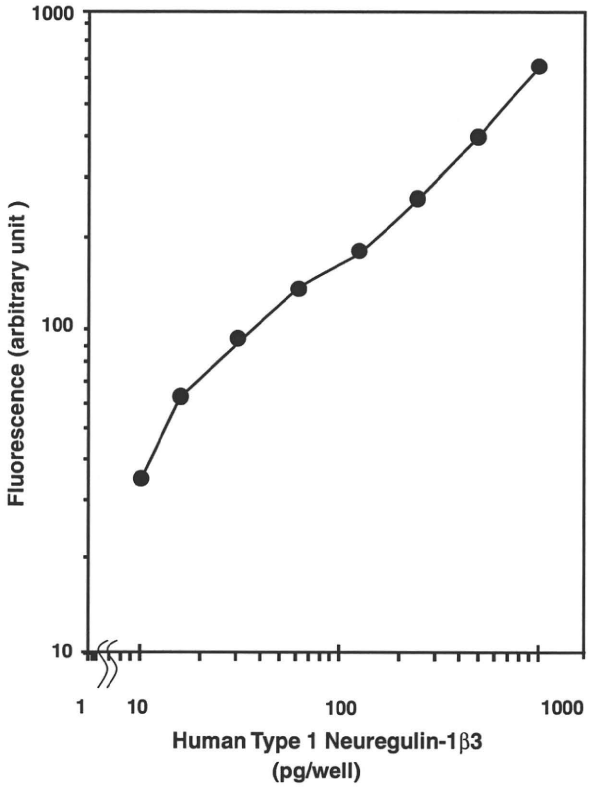

Fig. 1 A standard curve of ELISA with control type-1 NRG-1 peptide. Various amounts of human recombinant NRG1β3 (10–1,000 pg/well/100 μL) were applied to ELISA as a standard. Total immunoreactivity for NRG1 trapped by the primary antibody was determined using the guinea pig secondary anti-NRG1β1 antibody followed by detection with a β-galactosidase-conjugated antibody against guinea pig immunoglobulin. Enzymatic activity in each well was measured using the fluorogenic substrate MUG. The enzymatic product derived from MUG exhibits fluorescence at 450 nm with 365 nm excitation

(Nawa et al. 1995). The combination of these antibodies in ELISA generated a linear standard curve for concentrations of 10–1,000 pg/well for a soluble form of human NRG1β3 (Fig. 1). As NRG1 structurally belongs to the EGF family, we tested the cross-reactivity of this ELISA system to other members in this family, including EGF, HB-EGF, TGFα, betacellulin and epiregulin (Table 1). The cross-reactivity to these factors was <0.1% of the signal for type-I human NRG1β3. We also tested the reactivity of ELISA to the EGF domain of human NRG1 as well as other splice variants of human NRG1. Reactivity to the EGFβ1 domain was negligible (<0.01%), and that to the type-II and type-III variants was 61.0 and 7.2% of the levels seen for type-I NRG1 used as a standard, respectively. These results suggest that this ELISA primarily recognizes not the common EGF domain, but the Ig-like domain of NRG1, which is present in type-I and type-III NRG1, but not type-II NRG1. Using this novel ELISA, we measured

Table 1 Cross-reactivity to types I–III NRG-1 and other neurotrophic factors

Factor	Reactivity (%)
Human NRG1β3 (type I)	100
Human NRG1β3 (type II)	61.0
Human NRG1β3 (type III)	7.2
Human NRG1 core EGFβ1 domain	<0.01
Human betacellulin	<0.1
Human epidermal growth factor (EGF)	<0.01
Human heparin binding-EGF-like growth factor (HB-EGF)	<0.01
Human epiregulin	<0.01
Human transforming growth factor-α (TGF-α)	<0.01

Purified cytokines, growth factors and neurotrophic factors (10 ng) were applied to ELISA. The intensities of their signals were compared to those of human NRG1β3 (type I) in a standard curve

Table 2 Profiles of patients with schizophrenia and control volunteers

	Patients	Controls
Age (mean ± SD) (years)	32.7 ± 6.7	33.3 ± 6.9
Gender		
Men	20	28
Women	20	31
Duration of illness (mean ± SD) (years)	9.4 ± 5.7	
Age at onset (years)	23.2 ± 4.8	
Dose of antipsychotic medication[a]	716 ± 338	
Medication[b]		
Olanzapine (5–30 mg/day)	18	
Quetiapine (200–600 mg/day)	10	
Risperidone (2–9 mg/day)	6	
Perospirone (36–48 mg/day)	4	
Aripiprazole (12–18 mg/day)	4	
Haloperidol (4–12 mg/day)	2	
Others (2)[c]	2	

[a] Chlorpromazine-equivalent dose (mg/day)

[b] Some patients took multiple antipsychotics

[c] Other patients took clozapine (500 mg/day) or levomepromazine (25 mg/day)

According to DSM-IV diagnostic criteria, patients consisted of 13 disorganized types, 4 paranoid types and 23 undifferentiated types

Ig-like domain-containing NRG1-like immunoreactivity (Ig-NRG-LI) in human serum.

NRG1 immunoreactivity in sera of schizophrenia patients and control subjects

We obtained sera from schizophrenia patients ($n = 40$) and age- and gender-matched healthy volunteers ($n = 59$) (Table 2). The time of blood sampling, type of sampling